

GROWIAN ROTOR BLADES: PRODUCTION DEVELOPMENT,
CONSTRUCTION AND TEST

Hans Martin Thiele

Translation of "Growian Rotorblätter: Fertigungsentwicklung, Bau und Test", Bundesministerium für Forschung und Technologie, Bonn, (West Germany). Report BMFT-FB-T-83-111, June 1983, pp. 1-76

NATIONAL AERONAUTICS AND SPACE ADMINISTRATION
WASHINGTON D.C. 20546

JULY 1984

1. Report No. NASA TM-77479	2. Government Acquisition No.	3. Recipient's Catalog No.	
4. Title and Subtitle GROWIAN ROTOR BALDES: PRODUCTION DEVELOPMENT, CONSTRUCTION AND TEST		5. Report Date July, 1984	
7. Author(s) Hans Martin Thiele		6. Performing Organization Code	
9. Performing Organization Name and Address SCITRAN Box 5456 Santa Barbara, CA 93108		8. Performing Organization Report No.	
12. Sponsoring Agency Name and Address National Aeronautics and Space Administration Washington, D.C. 20546		10. Work Unit No.	
13. Supplementary Notes Translation of "Growian Rotorblätter: Fertigungsentwicklung, Bau und Test", Bundesministerium fuer Forschung und Technologie, Bonn, (West Germany), Report BMFT-FB-T-83-111, June 1983, pp. 1-76 (N84-11526)		11. Contractor Grant No. NASA 3542	
14. Sponsoring Agency Code		12. Type of Report and Period Covered Translation	
16. Abstract Development and construction of three 50 m rotor blades for a 3 MW wind turbine are described. A hybrid concept was chosen, i.e., a load carrying inflexible steel spar and a glass fiber reinforced plastic skin. A test blade was constructed and static loading tests, dynamic vibration tests and fatigue tests on critical welds as well as at the connection between spar and blade skin were performed. All tests results show good accordance with calculated values, and were taken into consideration during the construction of two rotor blades.			
17. Key Words (Selected by Author(s))	18. Distribution Statement Unclassified and Unlimited		
19. Security Classif. (of this report) Unclassified	20. Security Classif. (of this page) Unclassified	21. No. of Pages 79	22. Price

Bundesministerium fuer Forschung und Technologie

| 2 |

BMFT-FB-T-83-111

Technological Research and Development

-Non-Nuclear Energy Technology-

GROWIAN Rotor Blades:

Production Development, Construction and Test

by

Hans Martin Thiele

M.A.N. Augsburg-Nürnberg Machine Works

Incorporated

Division: NEW TECHNOLOGY

Munich

Branch Chief:

Dipl.Ing. Erich HAU

Project Manager:

Dipl. Ing. Hans Martin Thiele

June 1983

1. Report number 2. Type of report 3. Non-nuclear
BMFT-FB- T 83-111 Final report energy technology

4. Title of report

GROWIAN Rotor Blades: Production development, Construction and Test

5. Author

Thiele, Hans Martin

6. Project Completion Date

September 1982

7. Publication Date

June 1983

8. Organization Executing

M.A.N. AUGSBURG-NUERNBERG

9. Organization's Report No.

MACHINE WORKS INC.

10. Logistics ID No.

Division of New Technology

03E4324A

Dachauer Strasse 667

11. Number of Pages: 76

8000 Munich 50

12. Number of References: 1213. Sponsoring Agency14. Number of Tables: 3

Bundesministerium für Forschung

15. Number of Figures: 60

und Technologie (BMFT)

PO Box 200706

5300 Bonn 2

16. Supplementary Data17. Presented at (Title, Place, Date)18. Abstract

The project deals with the development, construction and testing of the 50m rotor blades for the GROWIAN 3 MW wind power plant. As a design concept a hybrid structure was selected, i.e. a load-bearing, untwisted spar stretches from the blade root to the tip; it is clad in a glass fiber reinforced plastic contour-true outer skin which assumes the aerodynamic loads. After construction of the test rotor blade, both static load tests and a dynamic vibration test were carried out. In addition, endurance strength investigations were carried out on critical weld seams of the spar, as well as load

tests on the blade skin/spar interface points. The results of these investigations will be taken into account in the fabrication of two rotor blades which will be put into operation at the GROWIAN installation in Kaiser Wilhelm Koog.*

(*Translator's note: Koog= an area of reclaimed land, similar to Dutch polder.)

19. Key Words

Rotor blades for large wind power plant GROWIAN

/4/

TABLE OF CONTENTS

	PAGE
1. Summary	5
2. Introduction	7
3. Rotor Blade Development	8
3.1 Aerodynamic design	8
3.2 <u>Engineering layout</u>	14
3.3 Description of construction	17
3.4 Load assumptions	23
3.5 Structural analysis	26
3.6 Twisting and flutter stability	37
4. Rotor Blade Fabrication	39
4.1 Steel spar	40
4.2 Skin	46
4.3 Installation	50
5. Quality Assurance	52
6. Transportation	55
7. Structural Testing	57
8. Project Execution	69
9. Conclusions	74

1. SUMMARY

The 03E-4323A Project concerns itself with the production development, construction and testing of the rotor blades for the GROWIAN wind power plant.

As part of this project, based on the "construction-ready" data from GROWIAN, the aerodynamic design was reworked and a modified structural concept was drafted. The result of these studies was the construction of a hybrid type rotor blade which has as the load bearing structure an untwisted, six-sided steel box spar which is clad in a glass fiber reinforced plastic shell which follows the aerodynamic profiling.

In the building of the test rotor blade there were checked out the manufacturing feasibility of the welded construction of the spar in connection with the adherence to fabrication tolerances and the quality of the weld seam and also the fabrication process for the plastic sheathing; the latter presented to some extent considerable problems due to the huge dimensions of the shell sections. Beyond this the test rotor blade was subjected to static load tests in a comprehensive test program, in order to demonstrate qualification of the component for later use. Since dynamic load tests were only to be carried out with a great expenditure of time and test engineering resources, duration strength tests were carried out experimentally with 10^7 stress cycles on test articles for the critical weld connections on the spar and for the shell/spar interfaces. All the duration strength values attained agreed with those basically established by computation.

The elasticities and deformations measured in the static tests showed good agreement with the computed values. The fracture test was broken off at 170% of the blade loadings arising in the load case $2.5 \times$ maximum since at some points on the spar the elasticities did not any longer proceed linearly. Before starting the static structural tests a dynamic oscillation test was carried out in which were measured the relevant characteristic frequencies and characteristic shapes. Here too good agreement was achieved with the calculated values.

All the findings in the construction of the test rotor blade and in the structural tests will be taken into account in the manufacture of rotor blades 2 and 3 for GROWIAN. During the test phase of GROWIAN, both rotor blades were fitted out with measurement sensors for purposes of making measurements. An evaluation of the mass distribution of the two blades based on the measured values showed that on rotor blade #2 compensation masses of about 60 kg had to be installed within the blade. This is to some extent attributable to differences in the metering equipment on the two rotor blades.

All computer documentation and the construction of the rotor blades was checked and/or monitored by the firm German Lloyd.

During the derivation of construction-ready data for the large wind power plant GROWIAN, two different rotor blade construction approaches were investigated.

Design I called for a blade structure of carbon fiber reinforced material from station R15 to R50. In design II, the outer length of blade was covered with carbon fiber reinforcing material from R30 to R50, while on the inner length of blade from station R30 to R10 a hybrid construction method was planned with a steel box spar as the load bearing structure and a glass fiber reinforced plastic sandwich configuration for attaining the aerodynamic form.

Accompanying static and dynamic load tests on components at full scale showed that, with respect to the projected construction of GROWIAN rotor blades of carbon fiber plastic, this was not feasible in the short term in this large a size. Here the problems are principally in the force initiation zone of the steel structure of the hub and in the fabrication process selected which has to assure a uniform quality of the material.

On the grounds mentioned above, it was decided to execute the rotor blades for the first GROWIAN plant in a hybrid construction mode. In June 1979, MAN-New Technology was placed under contract by the Nuclear Research Center, Jülich, on behalf of the Federal Ministry for Research and Technology, to execute Project 03E-4323A "Production Development, Construction and Test of the GROWIAN Rotor Blade".

The project included the following important objectives:

- re-working of the aerodynamic load assumptions for GROWIAN
- selection of a suitable fabrication process
- construction of a test rotor blade
- execution of structural tests with the test rotor blade
- manufacture of two rotor blades for GROWIAN

Project management, designing, construction and computations were carried out by MAN-NEW TECHNOLOGY; the spar was manufactured in the MAN plant at Gustavsburg and the shells by the firm Schempp-Hirth, Kirchheim. The structural testing was undertaken in collaboration with the IABG at Ottobrunn near Munich. The Jülich Nuclear Research Center employed the firm German Lloyd in Hamburg as monitor of the design and fabrication documentation and of manufacture of the rotor blades.

3. ROTOR BLADE DEVELOPMENT

/10/

3.1 Aerodynamic design and blade geometry

In the aerodynamic design of the rotor blade some compromises had to be decided for the aerodynamically optimal blade geometry, these with respect to the construction method chosen and in the interest of a cost-effective manufacturing method.

Here also, as in the preliminary design of GROWIAN, the laminar profile design of Prof. Wortmann, Series FX-77-W and FX-79-W were used. Three different profiles were used which are located at the following blade stations

R = 50	FX-79-151A
R=29.5	FX-77-W 258
R=15.7	FX-77-W 343

In between these profile sections it was smoothed linearly. In the blade root zone, below station R 15.7, the depth of profile was contracted down in the area of the last box section, such that thereby was created a FX-77-W profile with a 50% relative thickness.

The twist curve and the blade chord distribution over the spar length were calculated using conventional theoretical procedures based on the profile characteristics and layout data furnished by GROWIAN /1/. The hyperbolic shaped optimum blade chord distribution which resulted from these computations was replaced in favor of a double trapezoid shaped blade contour due to manufacturing considerations. The difference in performance behaviour between the optimum blade geometry and the double trapezoid blade turned out to be relatively small for the average roughness in the blade surface.

The optimization of the rotor blade geometry began with the following specified layout data:

Nominal performance	3 MW	Axis tilt	10°
Rotor radius	50.2m	Number of blades	2
Hub radius	8m	Design fast number	10
Cone angle	90°	Rotor RPM	18.5 min ⁻¹

Table 1 shows the geometric basic data for the blade geometry. In figures 3.1 through 3.7 the rotor blade smoothed outline is shown in simplified form together with the variation in the geometric parameters over the blade length.

Determinative for the fixing of the blade contour (blade chord distribution) was the endeavor to if possible accomodate the steel box spar untwisted in a dihedral rotor blade geometry (GFP outer shell). This yielded the gently bent double trapezoid plan (fig.3.0). The large relative thickness in the inside area was specified on structural grounds in order to guarantee the attachment to the circular blade root structure (rotor blade support).

Table 1: Geometric rotor blade parameters

Length (nominal).....	50.2m
blade support with hub connection.....	10.85m
Chord	
at blade tip.....	1.3m
at root.....	4.93m
Twist (non-linear).....	18°
Surface.....	105 m ²
Taper.....	0.26
Aspect ratio.....	15.4
Material.....	steel/GFP
Profile R 1.0.....	FX-79-W-151
R 0.6.....	FX-77-W-258
R 0.3.....	FX-77-W-243

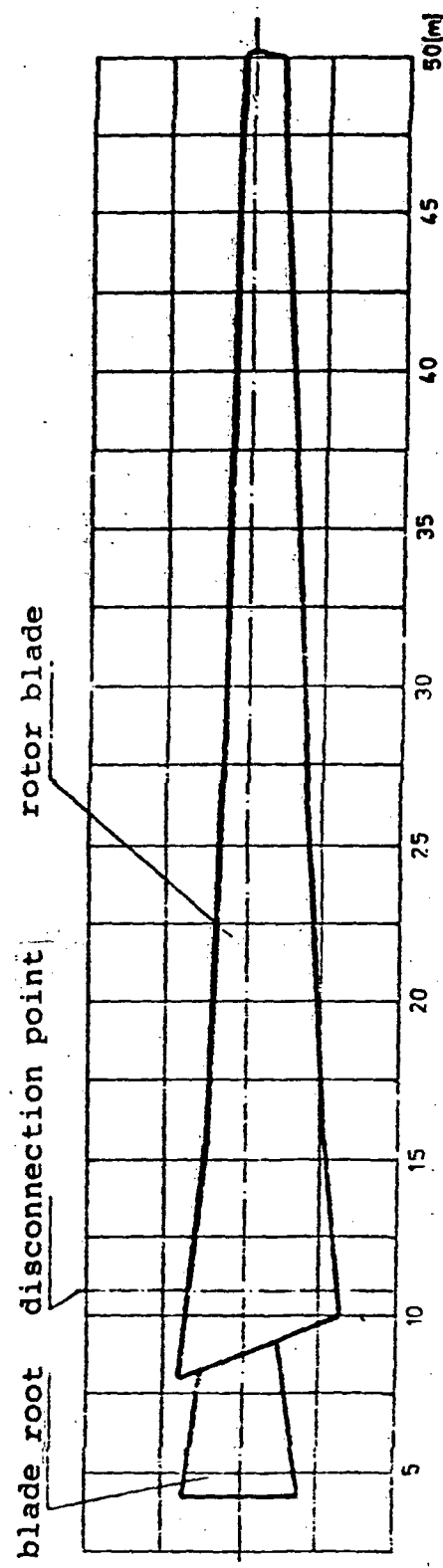


Figure 3.0 Rotor blade plan

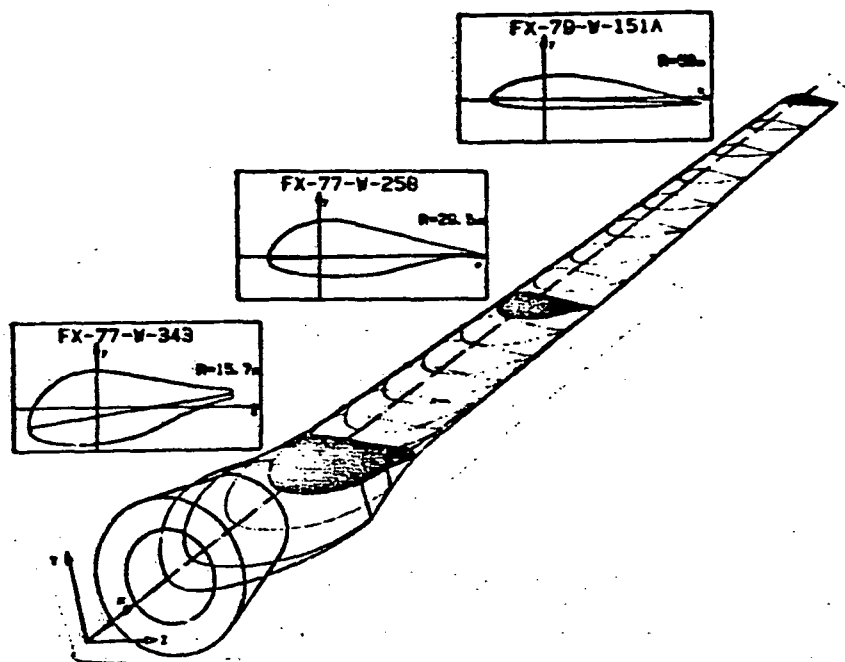


Figure 3.1 Rotor blade span

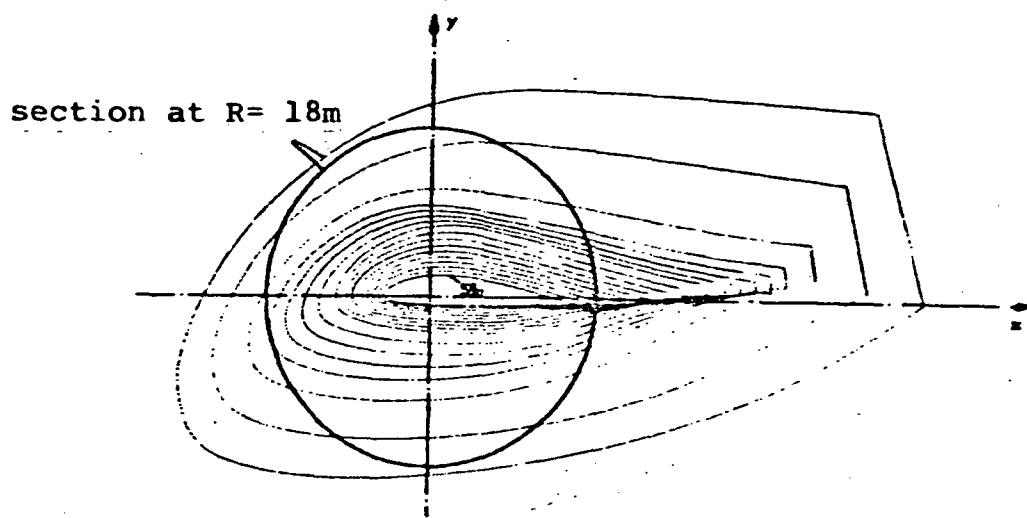


Figure 3.2 Rotor blade projection

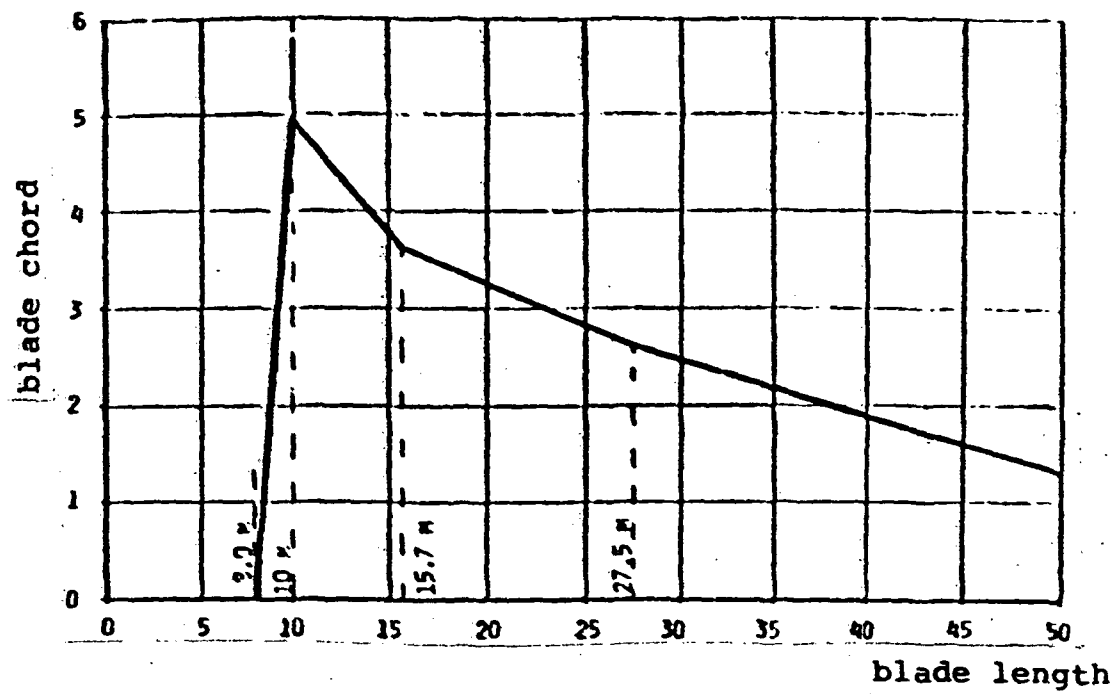


Figure 3.3 Blade chord curve

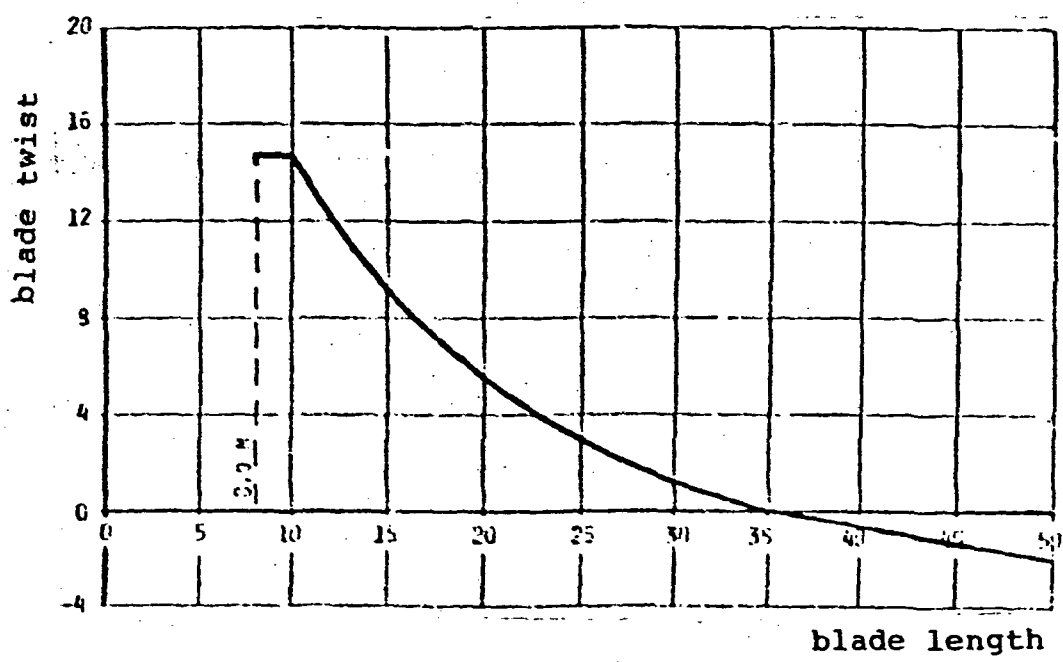


Figure 3.4 Twist curve

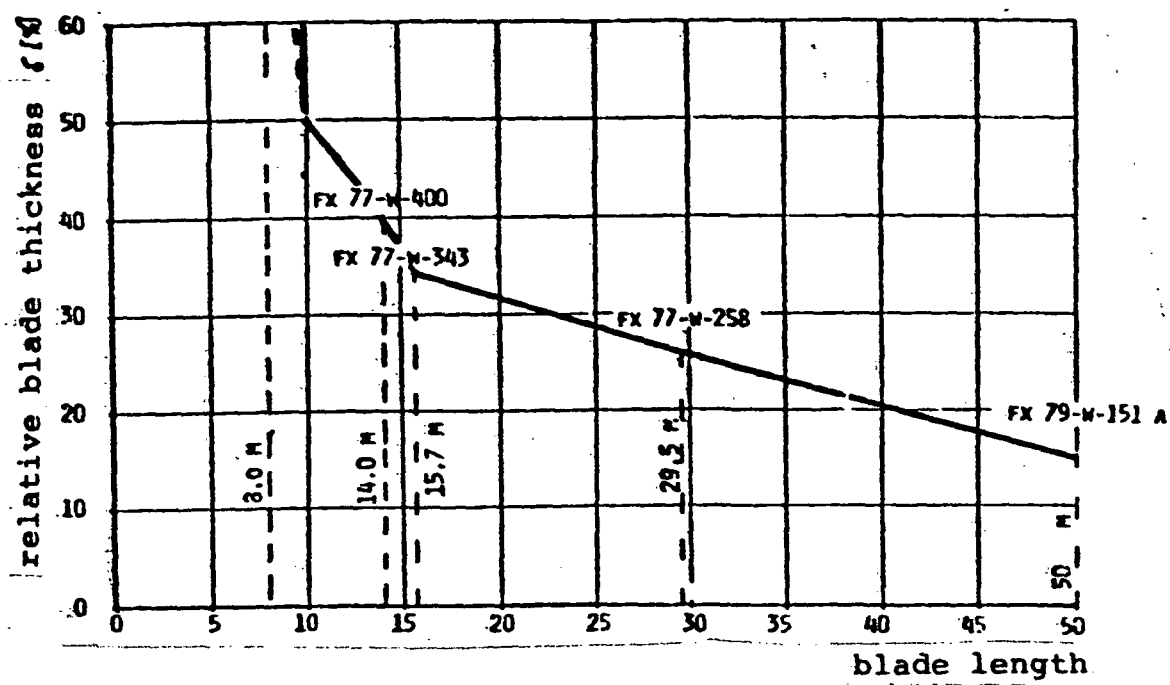


Figure 3.5 Relative blade thickness

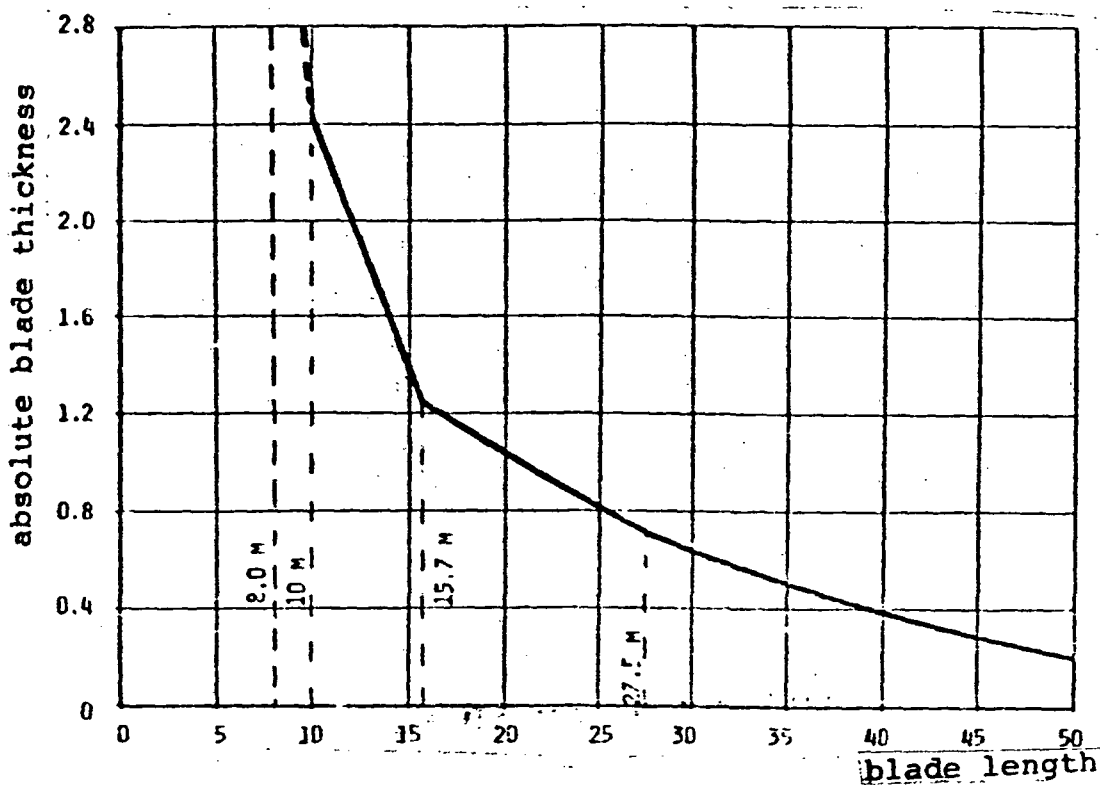


Figure 3.6 Absolute blade thickness

Sizing of the blade took place in accordance with the five defined basic load cases for GROWIAN. Additionally, a maximum allowable flexure of the blade at the blade tip of 2.9m was specified and a first characteristic bending frequency of higher than 0.8 Hz.

As an engineering concept there was selected a load-bearing steel box spar with a light plastic shell generating the aerodynamic loads. This concept was required in order to meet the specifications for the laminar profile in surface roughness and ripple.

Discovered as the optimum weight solution for the load bearing structure was an untwisted box spar with a six-sided cross section which reaches from the blade root out to the tip. Its positioning within the blade geometry was defined so that in the compression and tension chords the greatest uniformity is achieved in stress distribution during nominal operation. The shell/spar connection is produced by means of metal fittings.

The laminate setup of the glass fiber plastic shell was fixed for high rigidity (stiffness) in the profile circumferential direction and minimum stiffness in the vibration and oscillation direction, such that deformations of the spar can be endured by the shell without failing. Further boundary conditions for the shell design were sufficient pulling stability and resistance to hailstorm.

At blade station R 10.85m, the spar of the blade is welded to the blade root which contains the blade support. A two-point support installed on a trunnion on the cradle frame was selected in order to keep the bearing dimensions within tolerable size. The fixed bearing is located at station R 10m and the moveable bearing at station R 4.3m. Since up until now no reliable data could be generated on evidences of wear on the bearings resulting from the very restricted adjustment clearance per turn of the rotor, it was decided to design the structure such that both bearings can be changed out without disassembling the masthead.

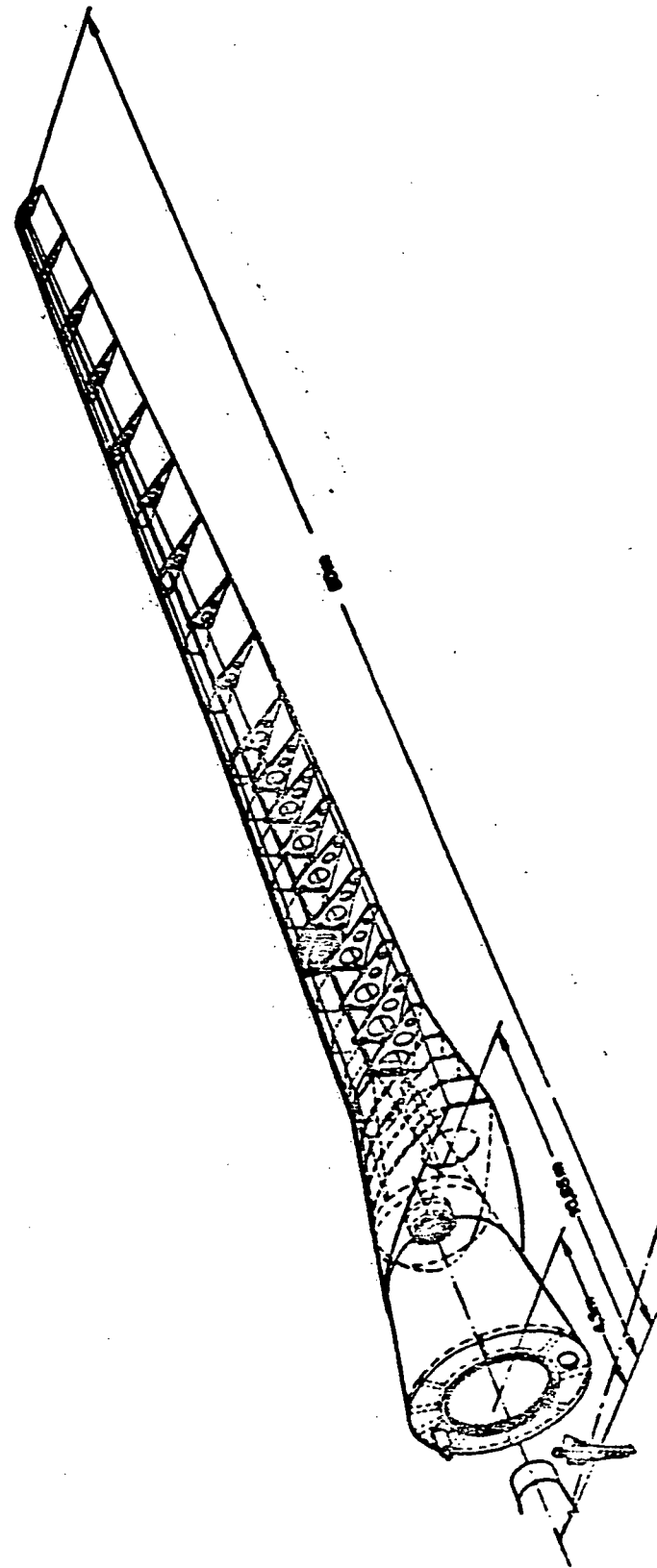


Figure 3.8 GROWIAN Rotor Blade

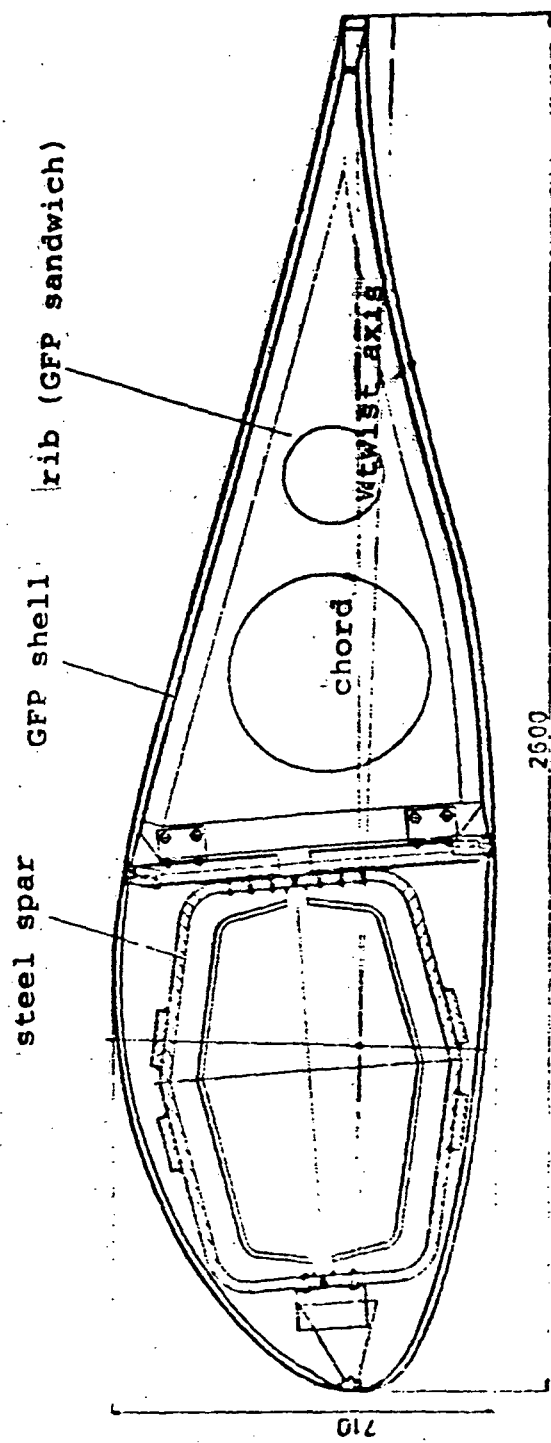


Figure 3.9 Rotor blade cross section at $\frac{r}{R} = 0.558$

3.3 Description of the construction

The untwisted steel box spar is carried out as a welded structure. (Figure 3.10) In the area of the blade root, its six-sided cross section merges smoothly into a circular form. In order to minimize the number of weld seams, the spar is composed of cold-formed half segments to station R 35m and quarter segments thereafter. In the inner area it is reinforced by half-ribs which are replaced by a central flange after station R 35m. Up to station R 35.3m the wall thickness amounts to 20mm; from there on it is reduced in steps from 15mm and 10mm down to 6mm at the blade tip. In the area station R24 to R32 the upper and lower chords of the box spar were reinforced by welded-on stringers.

To anchor the plastic shell of the blade skin three metal fittings, manufactured with a welded design, were screwed or riveted to the spar every 312.5mm. For each spar section, three fittings are installed, of which one is located in the nose area of the profile on the spar leading edge and two on the spar trailing edge. (Figure 3.9). In the center lies the spar from 10% to 38% of the profile chord.

The shells of the blade outer skin are executed in a glass fiber sandwich construction. The laminate consists of glass fiber fabric 0/90° and 45°/45° strata of different thickness. As a matrix was employed a cold-hardening epoxy resin system and as supporting material PVC hard foam.

In the area of the attachment points of the shell and the fittings roves of E-glass are inlaid in the shells in place of the hard foam. The sandwich thickness amounts to 16mm in the nose area and in the area of the box end 18mm. At all junction points the sandwich is joined and overlapped, cemented and fastened with bolts. For stabilizing the shape at the end box ribs are used which are cemented to the upper and lower shell and bolted to the spar fittings. They are arranged at intervals of 2.5m between blade stations R50 and R27.5 and of 1.5m between R 27.5 and the blade root.

The separation plane between upper and lower shell of the blade /20/ outer skin is the profile chord. For manufacturing engineering

reasons the overall blade skin is divided into five structural sections; the attachment points for these are located at stations R 37.5, R 27.5, R 15.6 and R 11.5. In the area of large blade chord between R 27.5 and R 10 m the upper and lower shells are once again subdivided in the longitudinal direction at the level of the attachment points on the spar trailing edge. (Figures 3.11 to 3.13).

The blade bearing support with the conical blade root structure is by definition part of the cradle frame of the hub. However, in the structural testing the blade bearing friction torque had to also be measured so that as part of this project a blade support was fabricated just for the test rotor blade.

The attachment point on the spar of the blade is located at R 10.85m. The bearing support is housed between stations R10.85 and R 4.3m. At R 10m there is a radial roller bearing unit as a fixed bearing having an outside diameter of about 500mm. Here both shear forces and centrifugal forces are absorbed. The moveable bearing at R 4.3m is in the form of a roller bearing and has an outside diameter of 1980mm. Both bearings are filled with oil as a lubricant. The lower structures of the bearing such as trunnion and blade root are so formed such that both structural components experience approximately the same deformation under load so as to avoid tilting of the bearing parts.

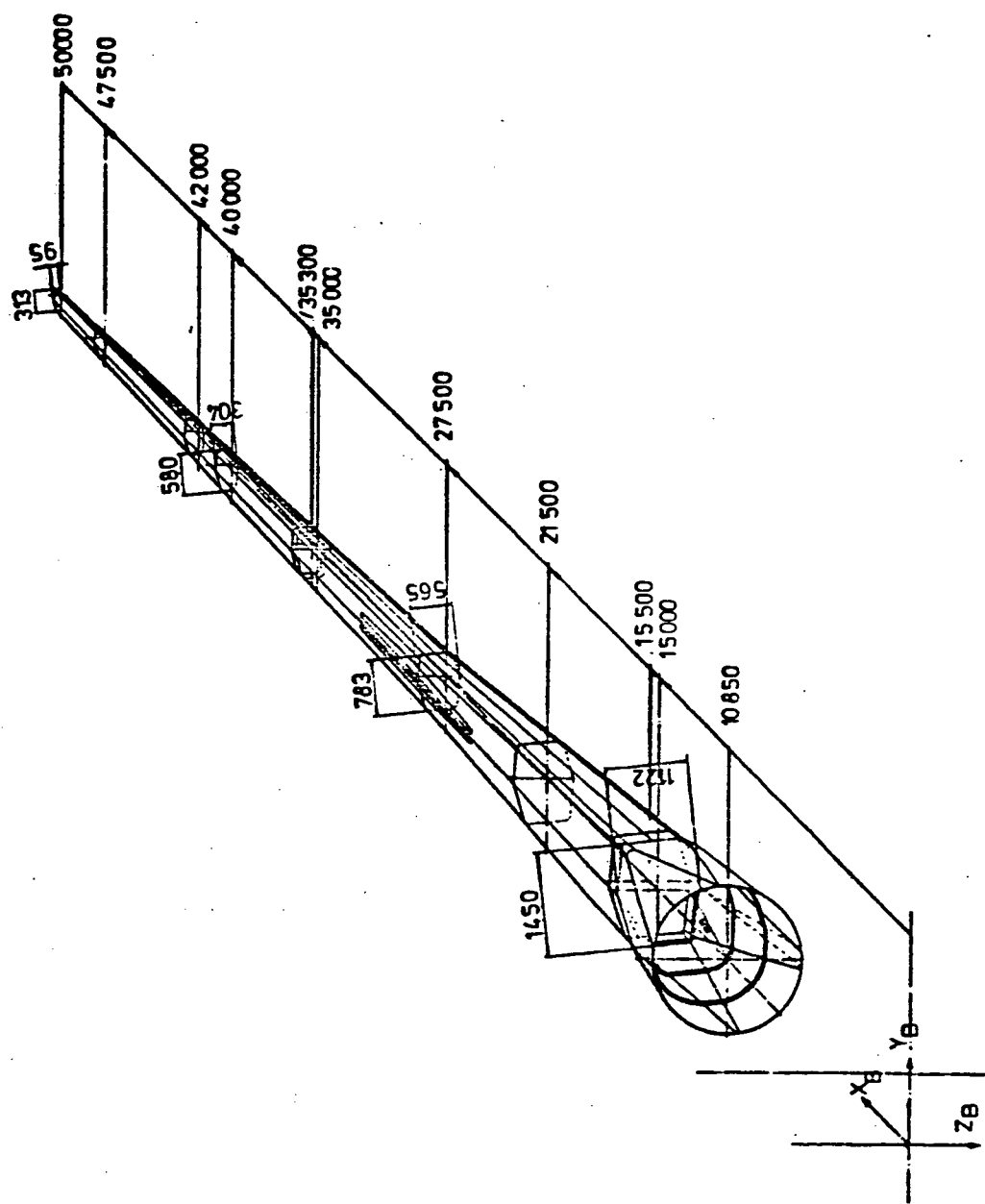


Figure 3.10 Steel box spar

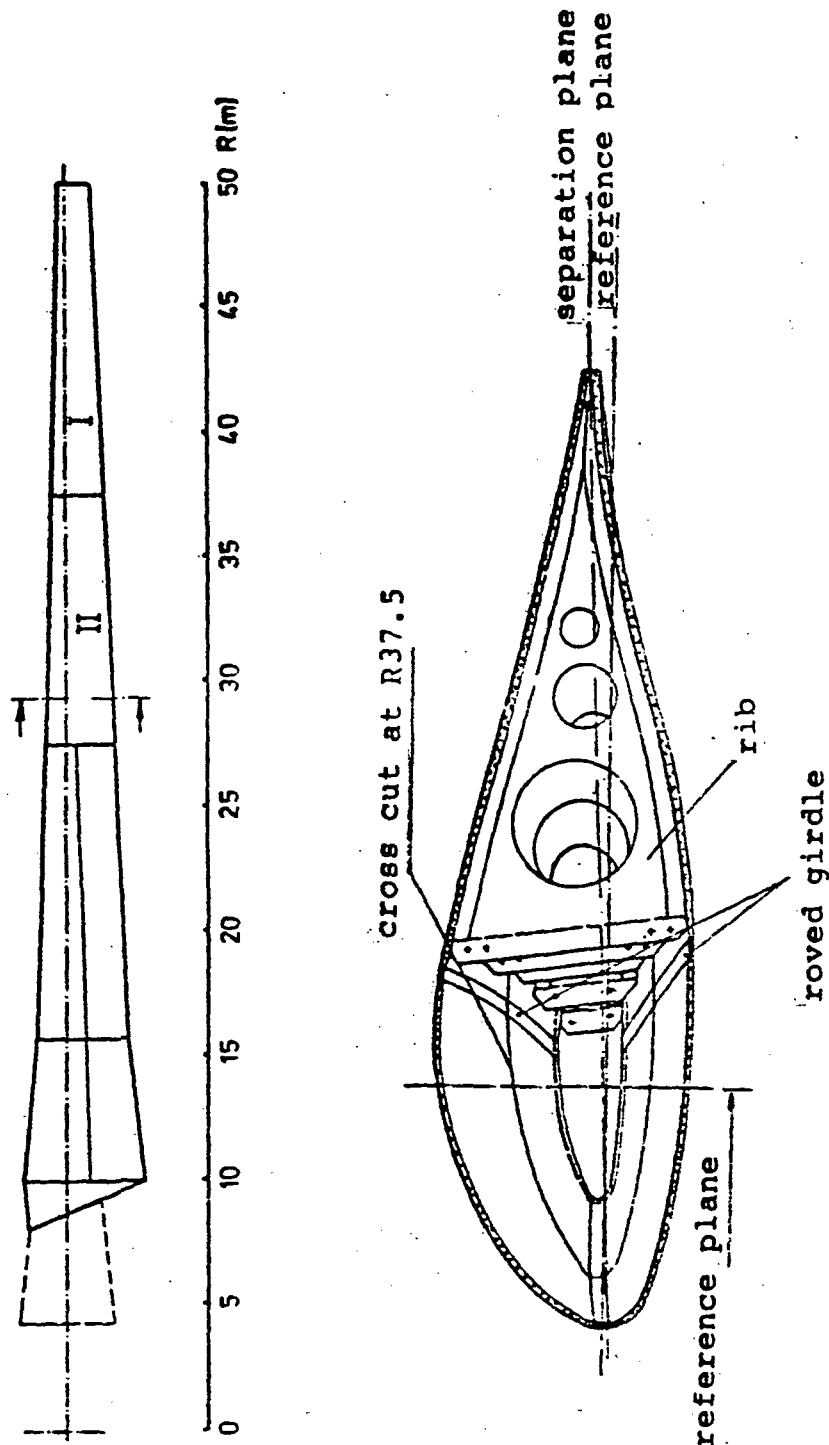


Figure 3.11 GFP-shell Structure section I and II

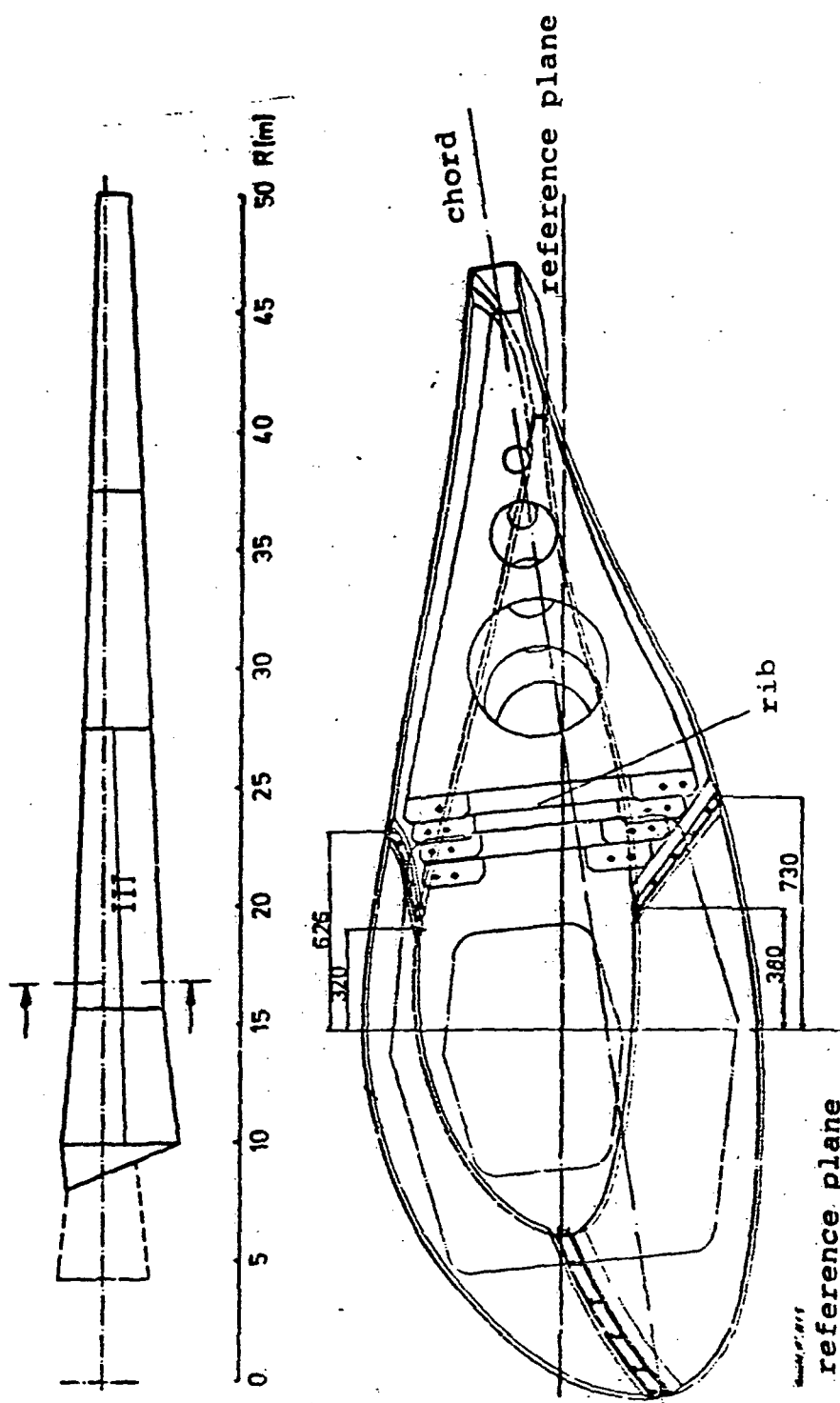


Figure 3.12 GFP shell Structure section III

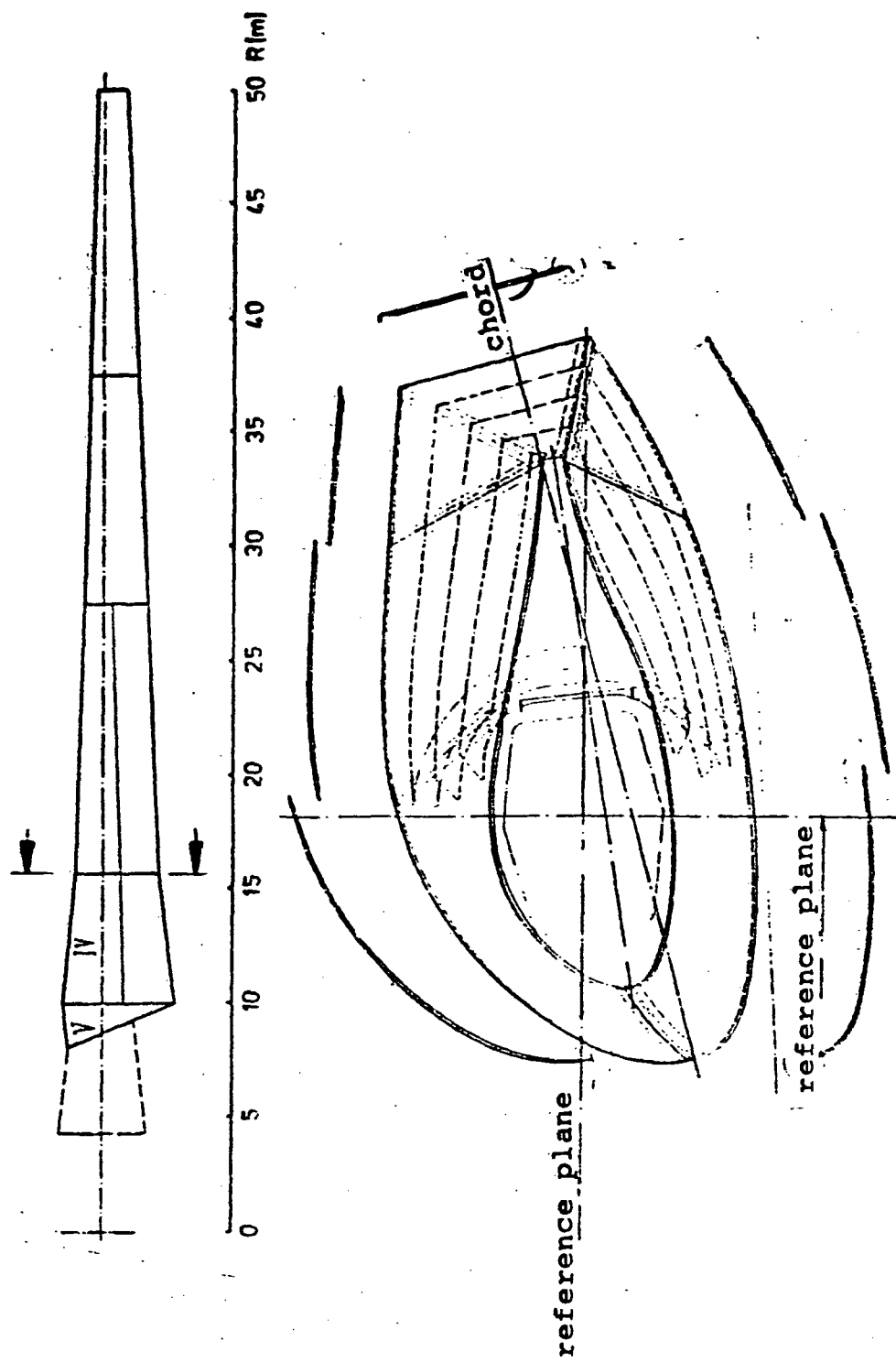


Figure 3.13 GRP shell Structure section IV and V

3.4 Load assumptions

The design and sizing of the rotor blades took place in accordance with the load assumptions described in the following. These load assumptions, to the extent that they involve environmentally conditioned influences, are based for the most part on the data published in this area up until now.

For GROWIAN the load assumptions have been subdivided into five basic load cases:

Load case 1: normal operation

Load case 2: wind gusts

Load case 3: start-up and braking procedure

Load case 4: rotor at rest

Load case 5: breakdowns

In these basic load cases, the wind has been assumed as steady and the air flow over the installation as undisturbed, i.e. ideal conditions. The consideration of more complex asymmetrical air flows, as well as the dynamic behaviour of rotor blades and the overall installation have been treated in the "Extensions" of these basic load cases. The definition of the load cases is exhaustively described in /12/.

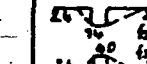
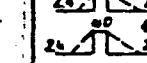
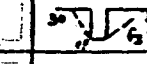
Each basic load case is subdivided into a series of individual load cases which are shown in Table 2.

The aerodynamic stresses in the load cases normal operation and wind gusts have been calculated with a digital computer program which were principally based on the extended blade element theory of Lissaman and Wilson /1/. Here velocity inductions both in wind and in circumferential direction along the blade were taken into account and superimposed on the inductions of the free tip vortices at the blade tip and blade foot. The aerodynamic load distributions is computed along the rotor blade as a function of rotor RPM's, wind velocity and blade angle of incidence with the rotor geometry of lift and drag polar curves and of the torsion moment behaviour. Here there were taken into account the axis tilt angle of the rotor, blade cone angle, pendular movement and blade pitch angle feed-back control.

/26/

These aerodynamic loads were superimposed on the antimetric components from the dead weight of the rotor blade over a rotation and on the mass forces from rotation speed and rotation speed changes, and on dynamic disturbances from tower wind shadowing and the ground boundary layer /3/, altogether into the total loadings on the rotor blades.

Table 2 Definition of the Load Cases per /12/

Load case	Nomenclature	Wind loads	RPM [min ⁻¹]	inc. [°/0,7°]	Load cycle
1	normal operation				$1,46 \cdot 10^8$
1.1	startup wind speed V_{c1}	$V_w = 5,4 \text{ m/s}$	16,65	- 2,5	$4,1 \cdot 10^7$
1.2	V_1	$V_w = 9,9 \text{ m/s}$	26,65	- 2,0	$3,64 \cdot 10^7$
1.3	nominal wind speed V_N	$V_w = 12,2 \text{ m/s}$	18,5	- 1,0	$4,2 \cdot 10^7$
1.4	V_2	$V_w = 18 \text{ m/s}$	18,5	-11,75	$2,3 \cdot 10^7$
1.5	shutdown wind speed V_{co}	$V_w = 24 \text{ m/s}$	18,5	-18,7	$3,1 \cdot 10^6$
2	wind gusts				
2.1	positive gust		18,5	- 1,0	104
2.2	negative gust		21,28	-16,9	10^6
2.3	extreme pos. gust		21,28	-16,9	50
2.4	" " neg. gust		15,73	-21,0	50
2.5	extreme neg. gust		21,28	-22,3	50
3	startup & brake procedure			Adj. rate °/s	
3.1	startup	$V_{c1} = 5,4 \text{ m/s}$ $V_N = 12,2 \text{ m/s}$ $V_{co} = 24 \text{ m/s}$	16,65 18,5 18,5	1 2 3	$1,8 \cdot 10^4$
3.2	emergency hydraulic shutdown	12,4 18 24	24 m/s 27 m/s 31 m/s	release 22,2 14/1	60
3.3	elect. fast control	12,4 16 24	24 m/s 27 m/s 31 m/s	release 21,28 14/1	60
3.4	normal shutdown	$V_{c1} = 5,4 \text{ m/s}$ $V_N = 12,2 \text{ m/s}$ $V_{co} = 24 \text{ m/s}$	16,65 18,5 18,5	0 0 0,5 °/s	
4	rotor at rest				
4.1	DIN 1055 wind velocity	$V_w = 45,6 \text{ m/s}$ $w = 30^\circ/-17,5^\circ$	0	- 90/0	
4.2	100 year wind	$V_w = 60 \text{ m/s}$ $w = 0^\circ$	0	- 90/90	
4.3	repair (DIN 1055)	$V_w = 45,6 \text{ m/s}$ $w = 90^\circ$	0	- 90/0	
5.	breakdowns				
5.1	ice buildup			0	- 90/0
5.2	lightning hit				
5.3	bird strike	$V_w = 1,5 \text{ m/s}$ $V_h = 15 \text{ m/s}$	18,5		

The derivation of profile loads, deformations and stresses in the blade structure was accomplished with a computer program developed for rotor blades of wind power plants.

The blade deformations and the profile loads were calculated in an iterative procedure for the quasi-stationary flow conditions using a linearized second order theory and the characteristic frequencies and characteristic shapes. /2/

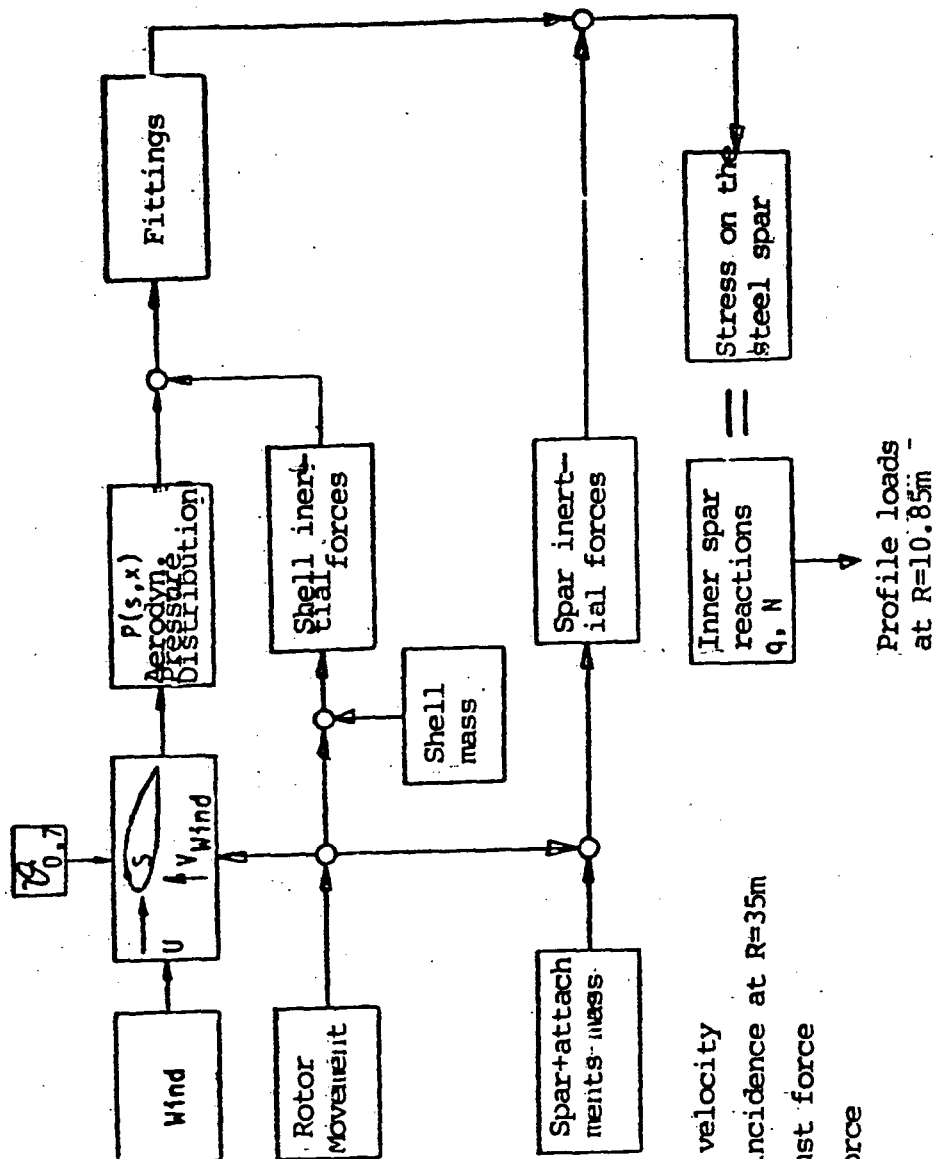
In idealizing the rotor blade, it was subdivided into three structural groups, the steel spar, the aerodynamic profiling (GFP shell) and the shell/spar attachment elements (tie-down fittings).

For the steel spar as a load-bearing structural component, the following assumptions were struck:

- The aerodynamic shell is moveable around its principal axis and thus adjusts itself to deformations of the steel spar. In the circumferential direction it is bend-resistant in order to maintain its profile shape /2/.
- All external loads and inertial forces are borne by the spar alone.
- In deriving the inertial forces and their points of attack, shell and fittings were all taken into account with respect to their masses and their distribution in the longitudinal and chord directions.

The GFP shell is stressed as a wing truss structure by the attrition of the aerodynamic loads into the spar and the deformation induced by the spar. In sizing the fittings, the profile loads on the three attachment points were derived from the aerodynamic loads, the volume forces (inertial and centrifugal force of the shell) as well as the compulsive forces from the elastic deformation of the blade (Figure 3.14).

In Figure 3.15 are shown the location of the principal axes, the center of rotation, center of shear, center of stiffness, aerodynamic pressure point and the center of gravity are given for the cross-section at blade station $R=35m$. The mass distribution shown in Figure 3.16 and the curve for the weight axes over the blade length in Figure 3.17 form the basis for the calculations. A comparison of the measured mass distribution with the theoretical values is included in Part 5.



u ... circumferential velocity
 α ... blade angle of incidence at $R=35m$
 q ... flow of the thrust force
 N ... flow of axial force

Fig. 3.14 Force flow diagram

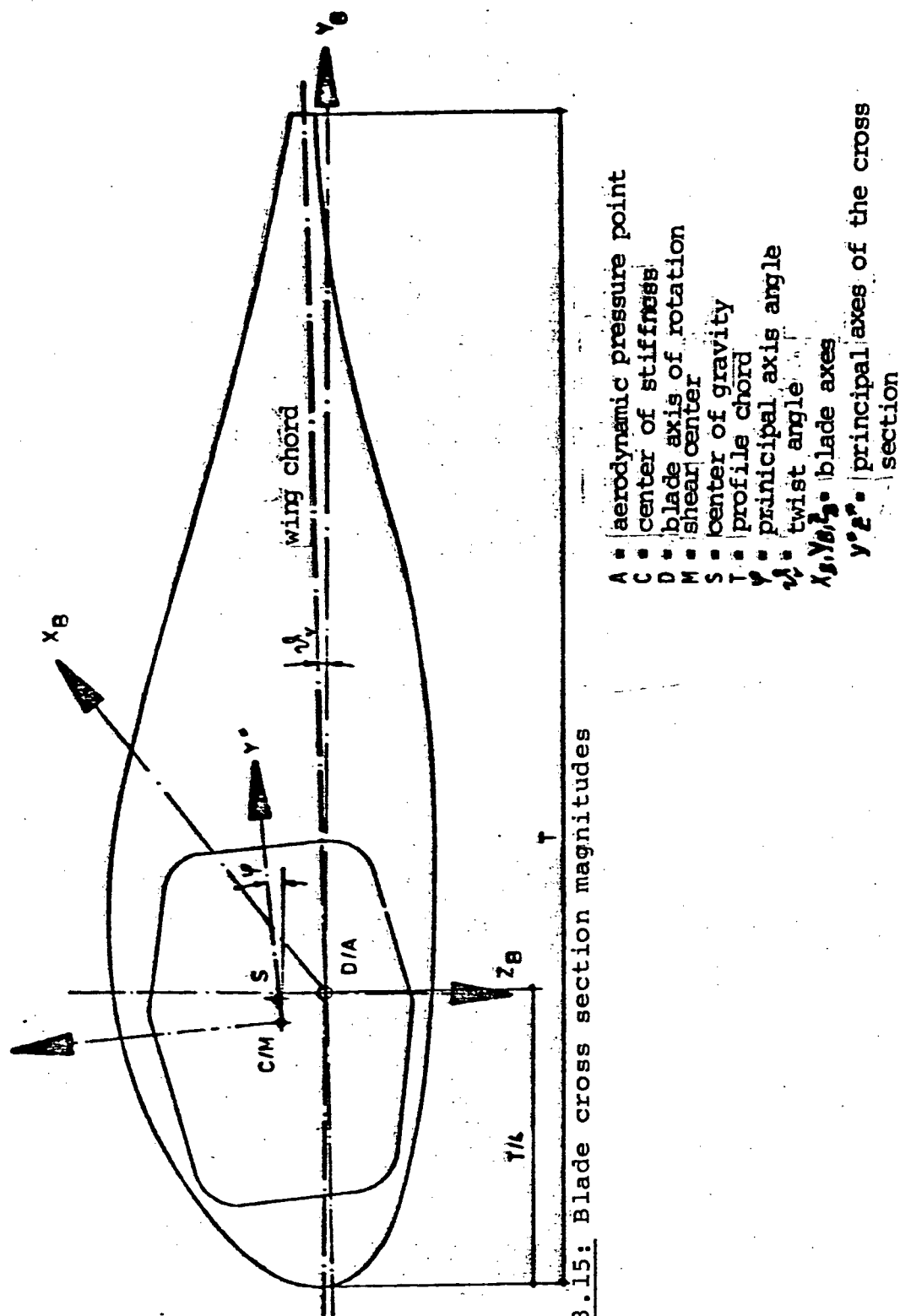


Figure 3.15: Blade cross section magnitudes

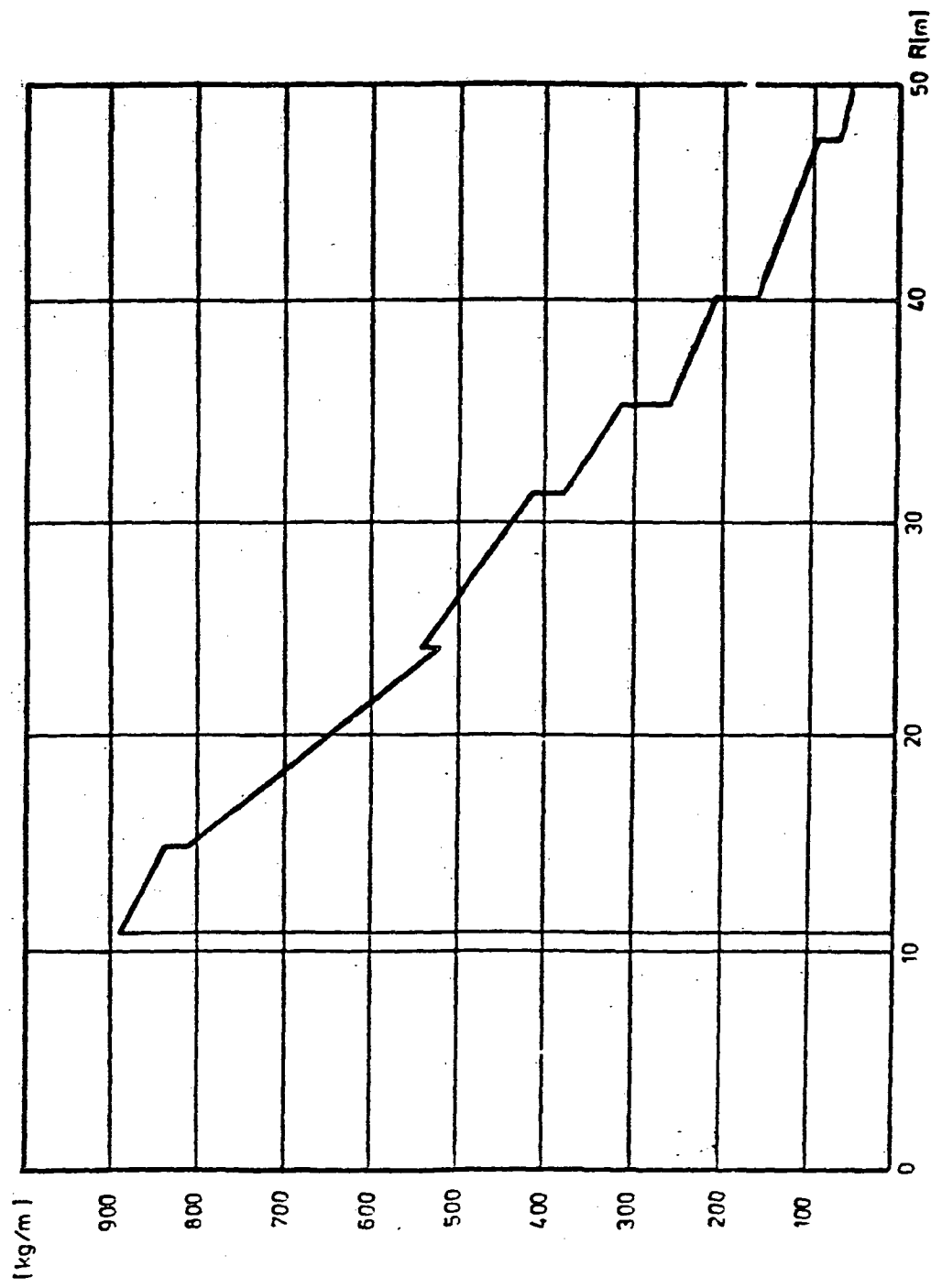


Figure 3.16: Mass distribution

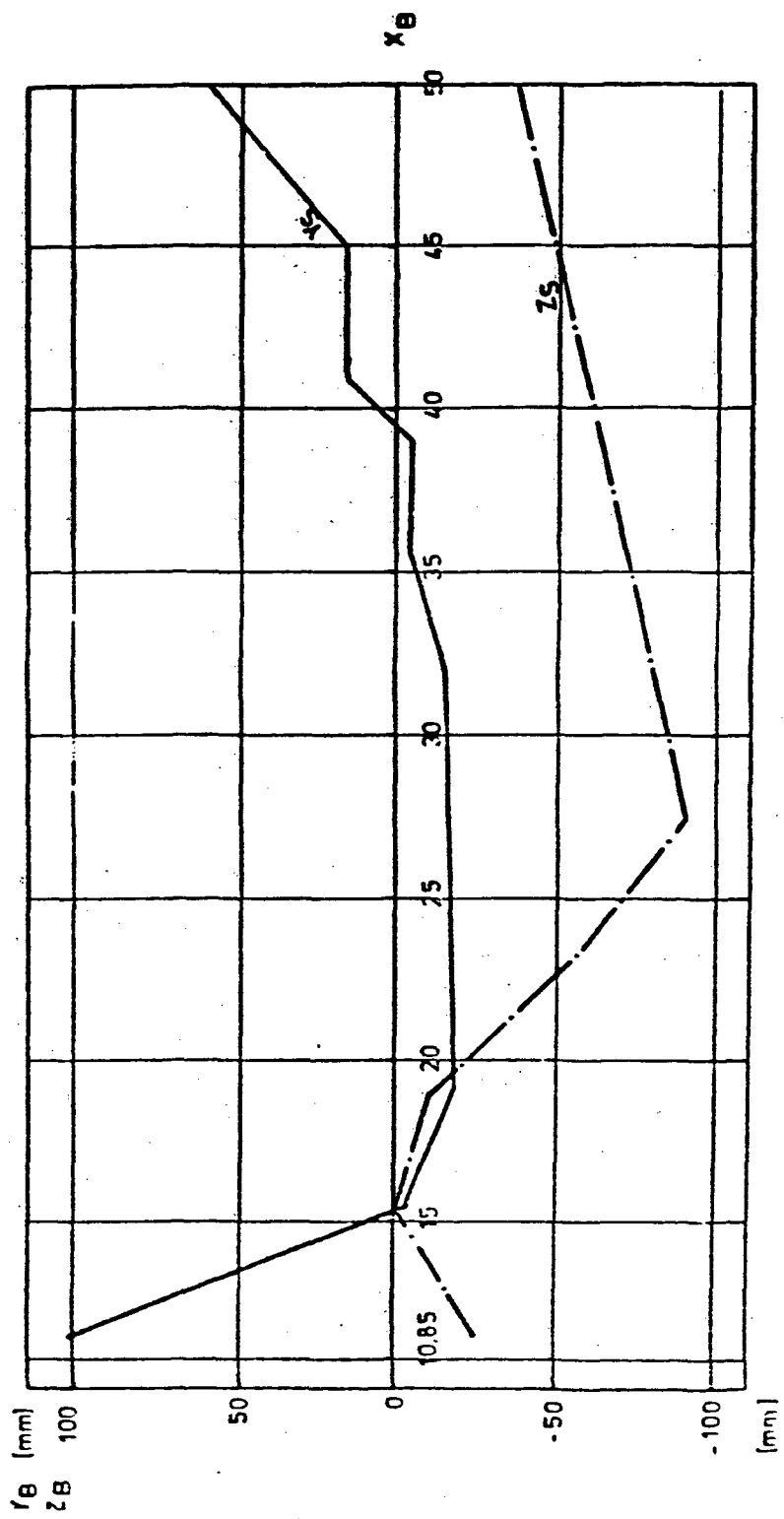


Figure 3.17: Location of the weight axes in the Y and X direction to the blade axis of rotation

For the spar, structural steel Qst 52-3 23 was employed /33/ having the following material characteristic values:

$$\begin{aligned} E &= 2.06 \times 10^5 \text{ N/mm}^2 & (\text{E-modulus}) \\ G &= 7.92 \times 10^4 \text{ N/mm}^2 & (\text{shear modulus}) \\ G_B &= 520 \text{ N/mm}^2 \\ \rho &= 7.85 \text{ g/cm}^3 & (\text{density}) \end{aligned}$$

The following material characteristic values are taken as a basis for the E-glass fabric of the outer skin for a unidirectional rove:

$$\begin{aligned} E_1 &= 316000 \text{ N/mm}^2 & (\text{E modulus // to the filament}) \\ E_2 &= 8030 \text{ N/mm}^2 & (\text{E modulus } \perp \text{ to the filament}) \\ G_F &= 4110 \text{ N/mm}^2 & (\text{shear modulus}) \\ \nu_{12} &= 0.332 & (\text{Poisson's ratio}) \\ \nu_{11} &= 0.0844 & (\text{Poisson's ratio}) \\ G_{112} &= 780 \text{ N/mm}^2 & (\text{fracture stress, tension // to the fiber}) \\ G_{113} &= 480 \text{ N/mm}^2 & (\text{fracture stress, pressure // to the fiber}) \\ G_{223} &= 40 \text{ N/mm}^2 & (\text{fracture stress, tension } \perp \text{ to the fiber}) \\ G_{223} &= 90 \text{ N/mm}^2 & (\text{fracture stress, shear}) \\ \rho &= 1.85 \text{ gr/cm}^3 & (\text{specific mass}) \end{aligned}$$

The sandwich core consists of Conticell foam C60 with the following properties:

$$\begin{aligned} E &= 60 \text{ N/mm}^2 & (\text{elasticity modulus}) \\ G &= 18 \text{ N/mm}^2 & (\text{shear modulus}) \\ G_{33} &= 1 \text{ N/mm}^2 & (\text{fracture stress, tension}) \\ G_{33} &= -1 \text{ N/mm}^2 & (\text{fracture stress, pressure}) \\ \tau &= 0.8 \text{ N/mm}^2 & (\text{fracture stress, shear}) \\ \rho &= 0.06 \text{ gr/cm}^3 & (\text{specific mass}) \end{aligned}$$

The stability certification for the steel spar was made on the /34/ basis of DIN 15 018 Part 1 "Cranes, Basic Data for Steel Supporting Structure, Computations".

For the general stress certification, for St 52-3, the following permissible stresses are produced:

a) Structural parts and all weld seams with longitudinal stressing:

Tension permissible $G_s = 270 \text{ N/mm}^2$

Pressure " $G_d = -240 \text{ N/mm}^2$

Shear " $T = 156 \text{ N/mm}^2$

b) Weld seams (only butt weld and K-seam special grade) with lateral stressing

Tension permissible $G_s = 270 \text{ N/mm}^2$

Pressure " $G_d = -270 \text{ N/mm}^2$

Shear " $T = 191 \text{ N/mm}^2$

c) Structural parts: Reference stress $G_r = 270 \text{ N/mm}^2$

d) All weld seams: Reference value $G_r = 270 \text{ N/mm}^2$

For the operational stability certification of the spar in normal operational modes 1.1-1.5, DIN 15 018 was again followed. The permissible stresses were, however, in this case reduced, in consideration of the special operating conditions of a wind power plant, by a factor of $\zeta = 1.2$. In this way, for example, reductions in endurance are eclipsed by the load case superimpositions.

The weld seams of the spar were so manufactured that only roughness cases of K2 or better can arise. This means the execution of butt and K seams in special grade materials in the case of lateral stressing.

With roughness K 2 and stress group B 6, for St 52-3 there is /35/ produced a basic value for the permissible stresses of $G_d (-1) = 52.5 \text{ N/mm}^2$ for the operational stability certification.

On the basis of the above mentioned permissible basic value, the permissible overstresses $G_o (\chi)$, which are dependent on the boundary stress ratio $\chi = \frac{\text{min}_o}{\text{max}_o}$, are computed according to DIN 15 018 with the formulae given there.

The findings of the stability analysis showed that in load case 1.3 (nominal operation) the highest normal stress occurs with $\sigma = 147 \text{ N/mm}^2$, and the smallest safety margin is achieved in load case 1.5 (shutdown, wind speed).

In the general stress certification, in load case 2.5 the highest normal stress was attained with $\sigma = 266 \text{ N/mm}^2$.

In Figures 3.18, 3.19 and 3.20 are shown the stress amplitudes over the rotor rotation in load cases 1.3 and 1.5 for a node point

of the spar cross section at station R 41.0m, and also the transition from load case 1.3 to 1.5.

In addition to the stress analysis, the characteristic frequencies and shapes of the rotor blade taking into account the blade adjusting linkage. /5/

The stiffness distribution shown in Fig. 3.18 was the basis for the computations. Figure 3.21* shows the computed characteristic frequencies over the rotor RPM with an elastically restrained blade at station R = 4.3.

* Transl. note: in error?. should be 3.22.

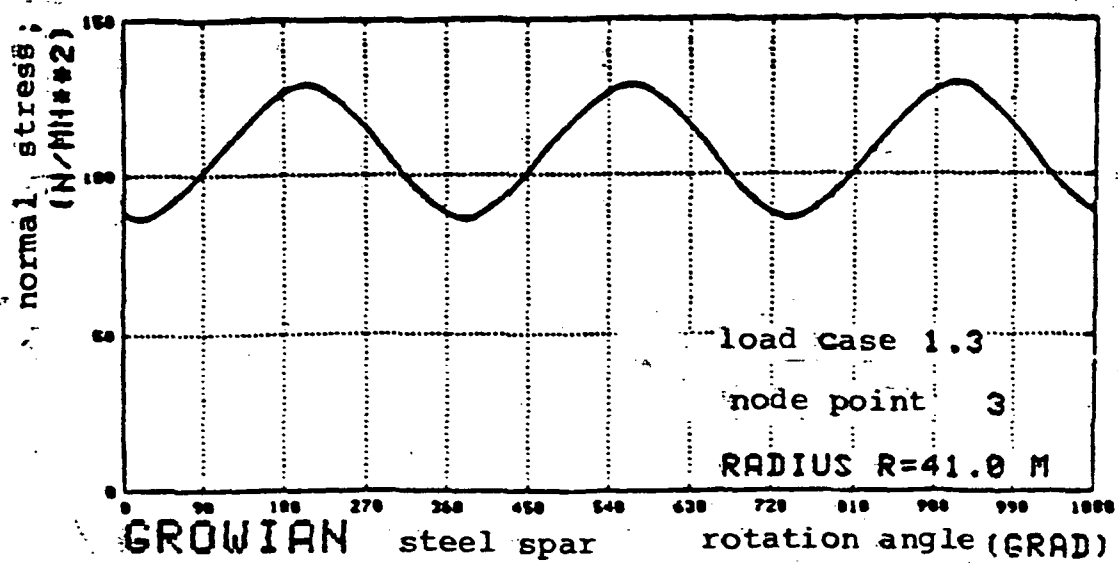


Figure 3.18. Stress curve in the spar over a rotor rotation load case 1.3

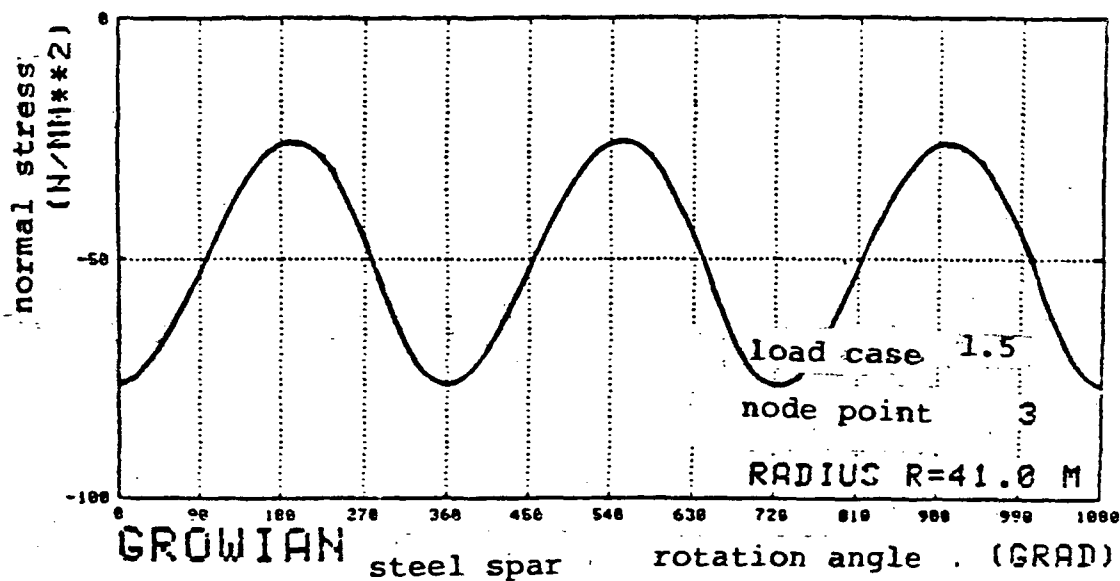


Figure 3.19. Stress curve over a rotor rotation, load case 1.5

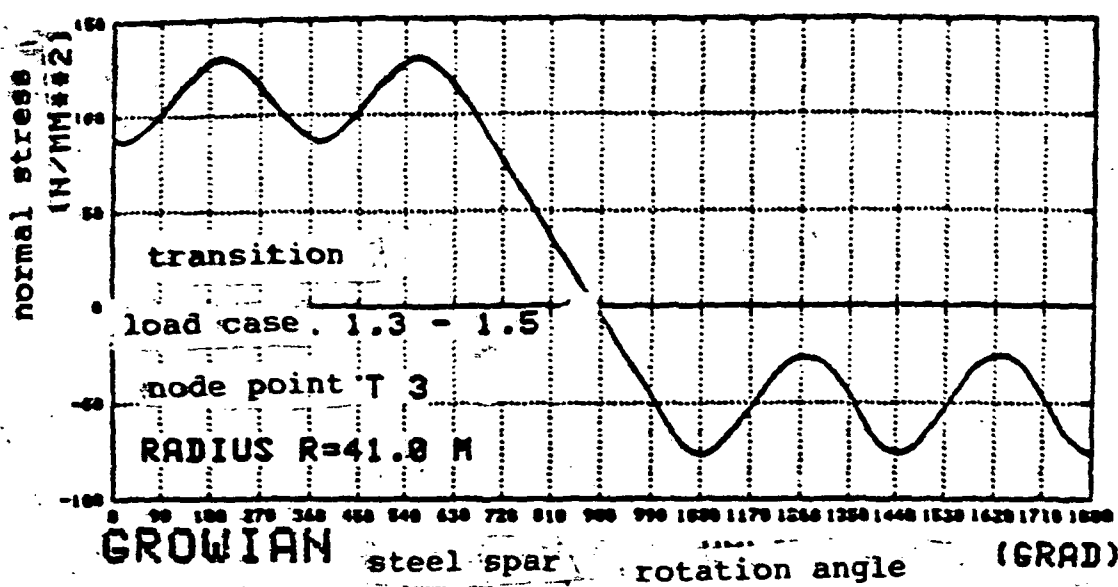


Figure 3.20 Transition of the stresses from load cases 1.3-2.5

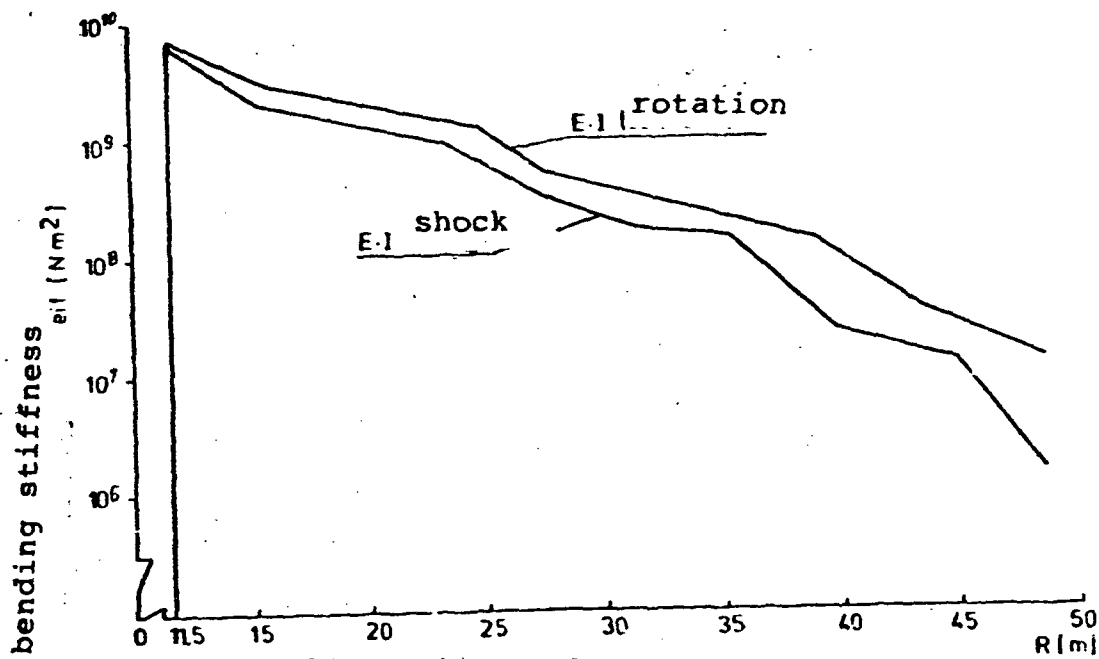


Figure 3.21 Stiffness distribution

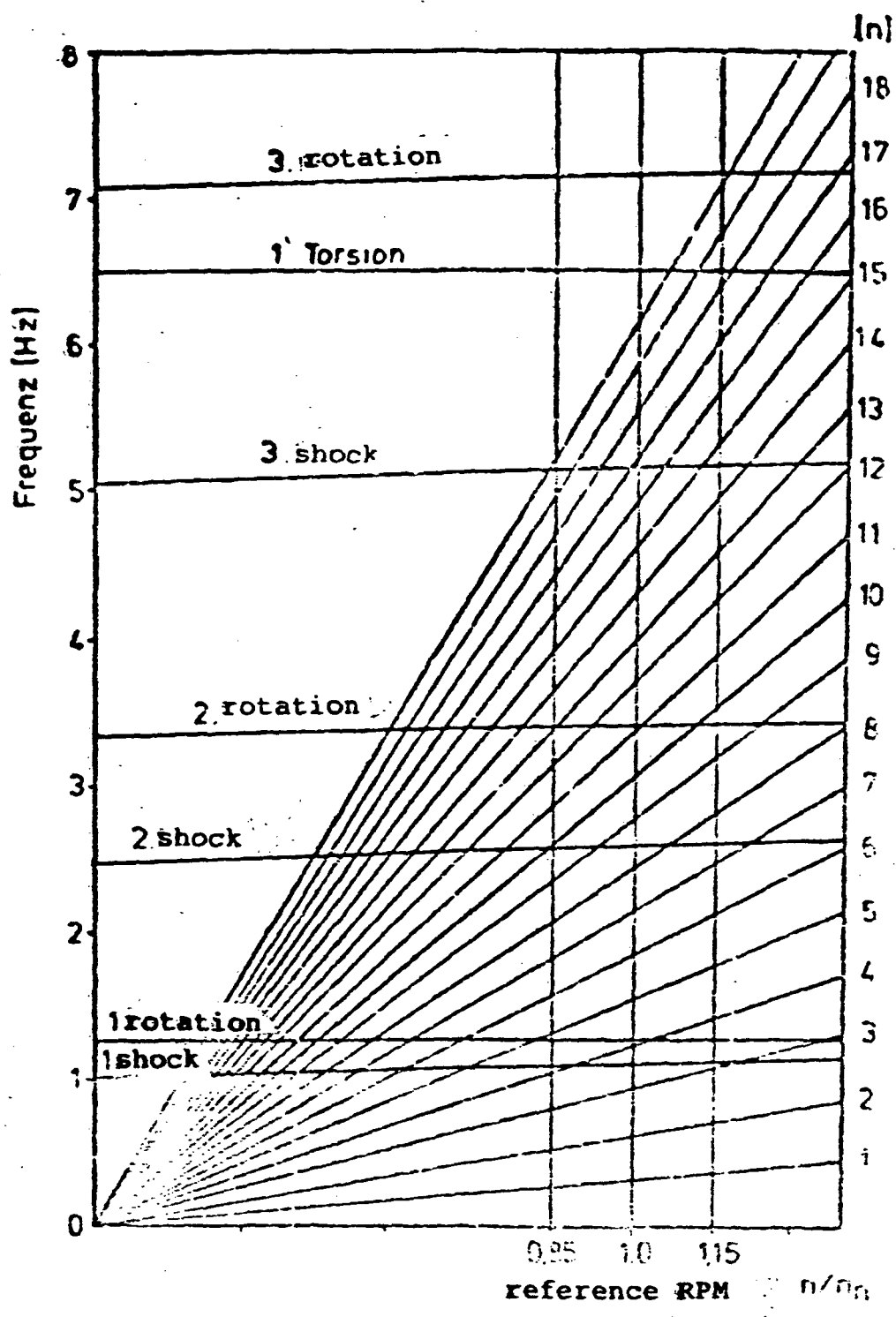


Figure 3.22 Blade frequencies over RPM

3.6 Twisting and flutter stability

On account of the torsion-yielding restraint of the rotor blade and an associated enhanced coupling of the bending shock and torsion frequencies, an investigation into flutter behaviour of the rotor blade became mandatory /6/.

Investigation of the flutter behaviour was carried out with the nine lowest elastic characteristic shapes of the rotating rotor blade at various RPM's. As boundary condition, the rotor blade, in the symmetrical case, was elastically restrained at blade station R 4.3.. In this way the influence of the cradle frame, adjustment linkage and blade adjustment pin elasticities was simulated. In the antimeric case, the rotor blade was arranged to oscillate at station R = 0, taking into account the blade angle return control. The elastic area between R = 0m and R = 4.3m was modeled with supplemental spring rigidities.

In Figure 3.24 is portrayed the curve for the damping magnitudes and frequencies for the antimeric case and in Figure 3.23 for the symmetrical case. The terms SL 0-4 reproduce the characteristic shape in the shock direction and T is for the twisting. All damping values up to rotor RPM $n = 1.4n$ nominal remain in the positive range so that here no instabilities arise.

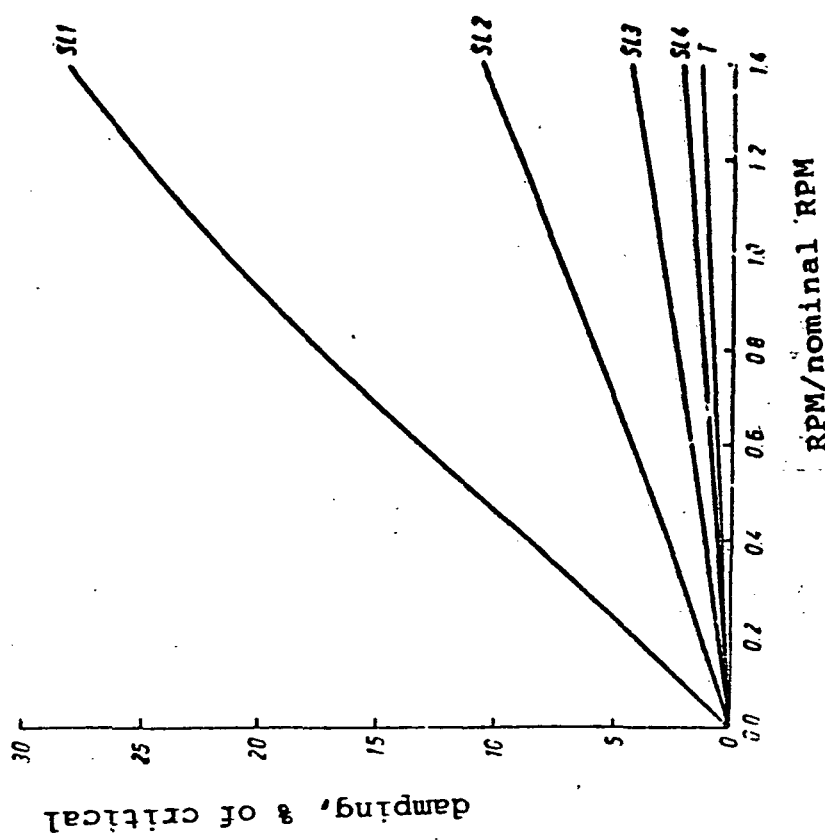


Figure 3.23: Curve of damping against RPM in the case of elastically suspended rotor blade

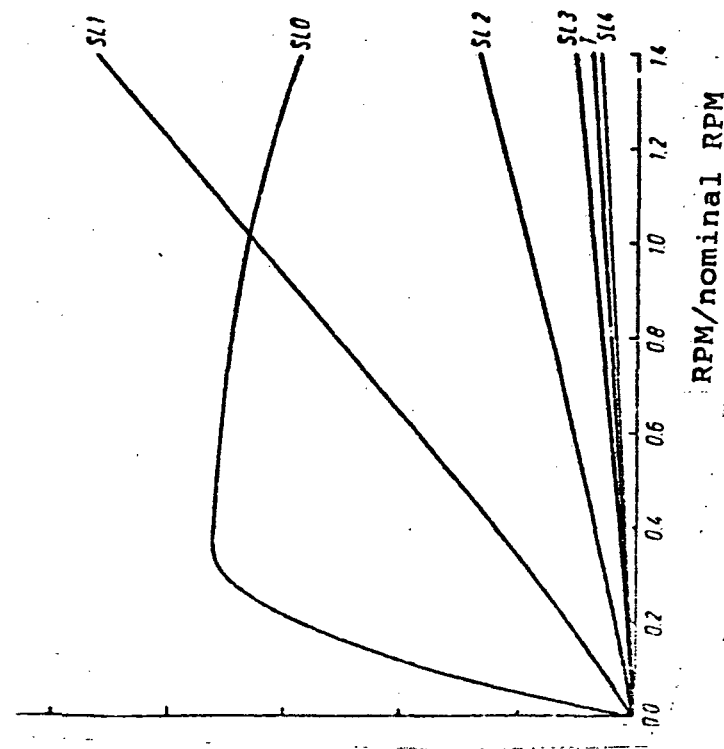


Figure 3.24: Curve of the damping against RPM in the case of oscillative suspended rotor blade

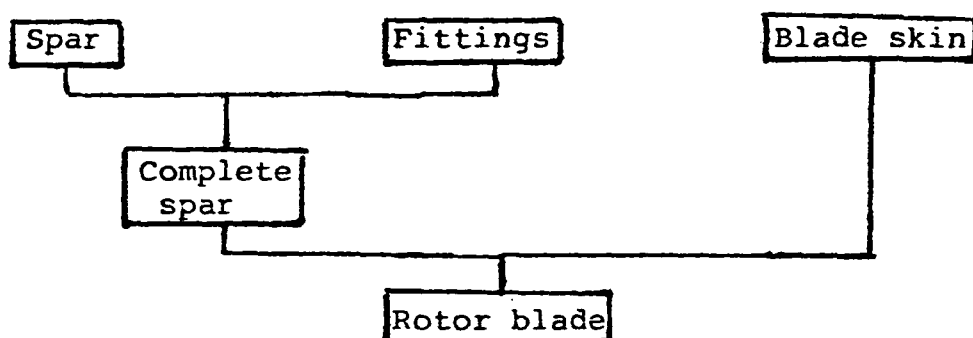
4. FABRICATION OF THE ROTOR BLADE

Since in this project the construction of three rotor blades was planned, fabrication techniques were selected which required the smallest possible commitment of expensive special equipment such as special fixtures, molds, press dies etc. This measure required, however, special capabilities for manual fabrication by the plants in order to meet the small structural tolerances.

Given these prerequisites, the following fabrication scheme was realized:

Spar	<ul style="list-style-type: none"> ● welded construction ● low commitment of fixtures ● reduction of weld seams to a minimum
Blade skin	<ul style="list-style-type: none"> ● GFP sandwich construction ● manual application into shaping pans ● fabrication of the largest possible shell sections ● simplicity of installation
Fittings	<ul style="list-style-type: none"> ● simple welded construction ● process variable in order to equalize tolerances between spar and skin

With the subdivision into three structural groups, parallel fabrication of the individual components was possible according to the following manuaufacturing plan:



The strict requirements for size accuracy in the spar geometry, particularly on the junction points of the spar sections required a slipway (Figure 1) in which the geometry of the spar could be checked using templates. In order to keep the weld seams to a minimum, the steel plate was chamfered into $\frac{1}{2}$ and $\frac{1}{4}$ shells with a length up to 7.5m. (Figure 2)

This work procedure was not carried out with press dies, but rather step-by-step free-form using a pressure sheath, cold-formed until the final contour is achieved. This procedure is frequently used in ship and steel frame construction.

Following this work procedure, half-ribs are welded into the spar shell (figure 3). Then comes the mechanical work on the junction points in the longitudinal direction and the welding together of the half-shells into a spar section (Figure 4). After matching up the butt joints, the spar sections for R 10.85-R 35 are welded together (Figure 5).

Next, in the spar area R 35 to R 50m the $\frac{1}{4}$ -shells are joined together into $\frac{1}{2}$ -shells, and then the $\frac{1}{2}$ -shells of the individual sections are bound into a complete spar half by butt welds. After matching up the long-cross, the longitudinal welds were applied in both top and bottom of the spar contour (Figure 6).

The transition from the six-sided cross-section of the spar into a circular shape at station 10.85 takes place smoothly in accordance with the procedure described for the manufacture of the shells.

Special care was taken in the execution of the welding jobs since here, with respect to the operational stability of the spar,

roughness condition K2 in DIN 15 018, or better, must be adhered to. So all butt welds which lie at an angle to the load direction were worked down to the level of the plate on both sides and all other weld seams were ground down free of roughness.

During the fabrication, the individual structural components /43/ of the spar were covered on the outside and inside with a corrosive protective base coat of zinc silicate base which is supplemented with a covering coat of epoxy-resin base on the spar outside after installation of the attachment fittings. The interior of the spar was partitioned by bulkheads below R.23 m.

The attachment fittings are manufactured in parallel with the spar fabrication and then fitted in using the slipway and attached to the spar (Figure 7)

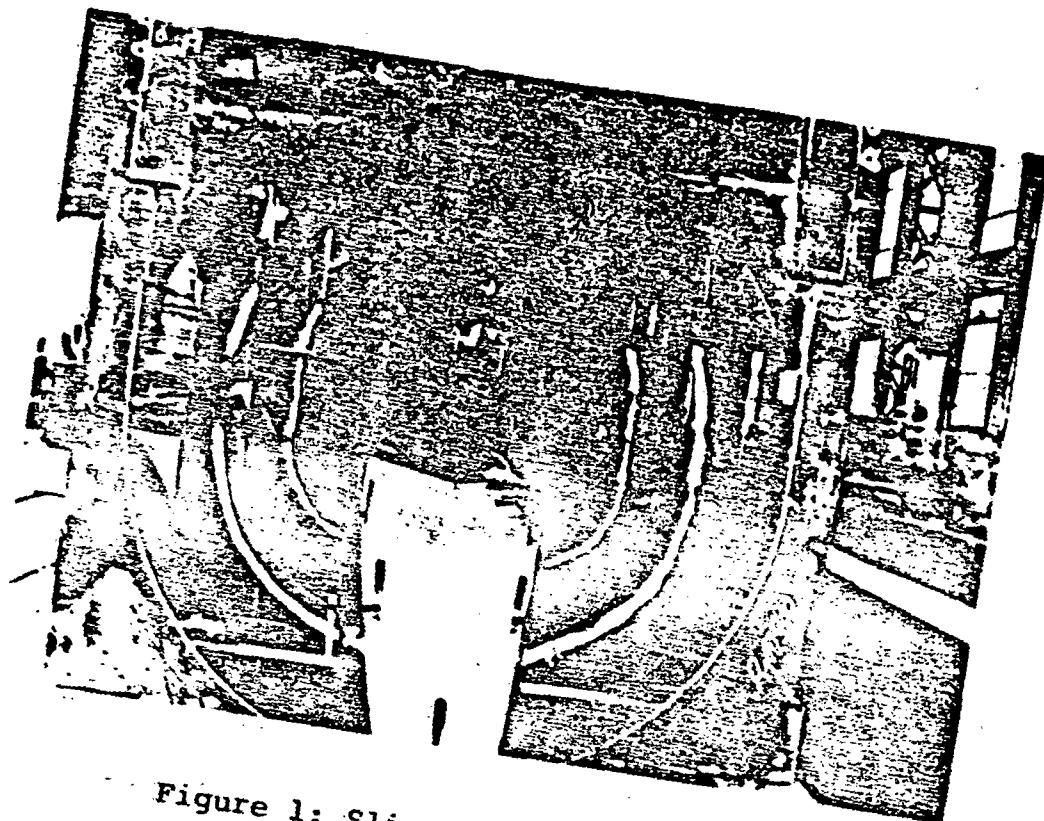


Figure 1: Slipway

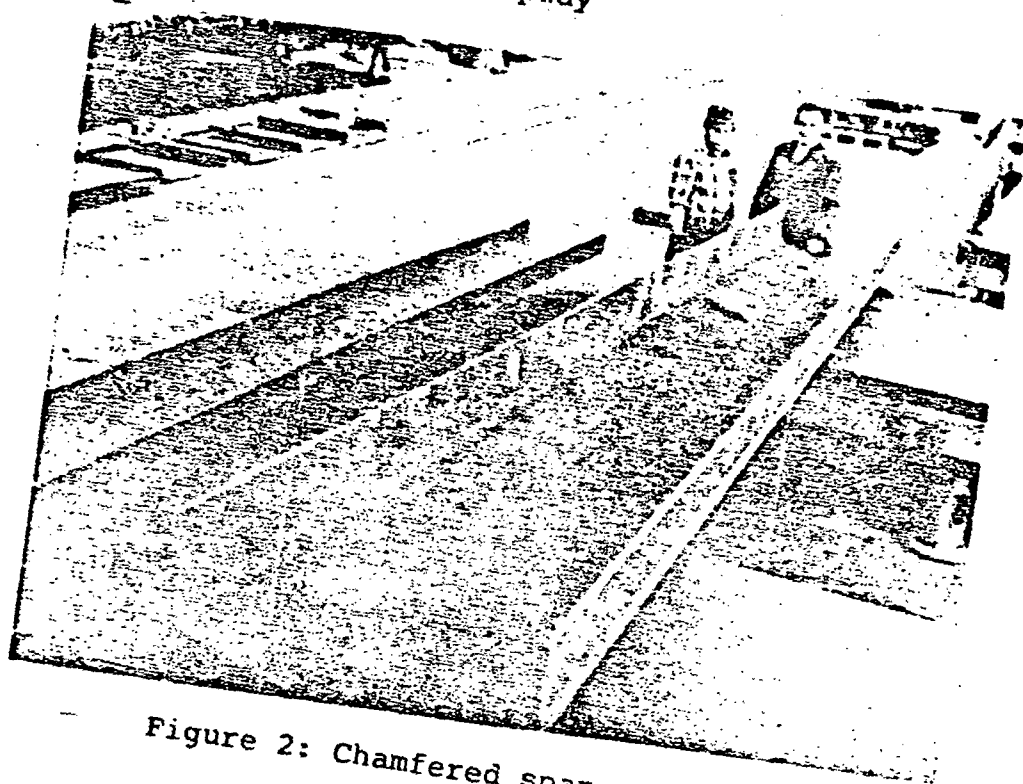


Figure 2: Chamfered spar profile



Figure 3: Spar profile stiffened with ribs

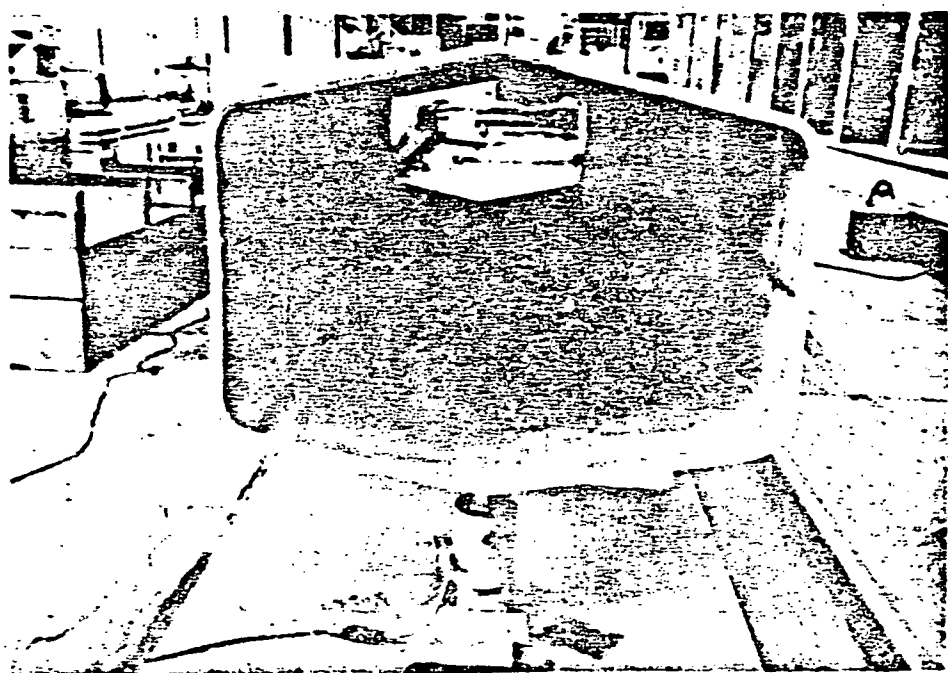


Figure 4: Spar section R 15.5-R 21.5

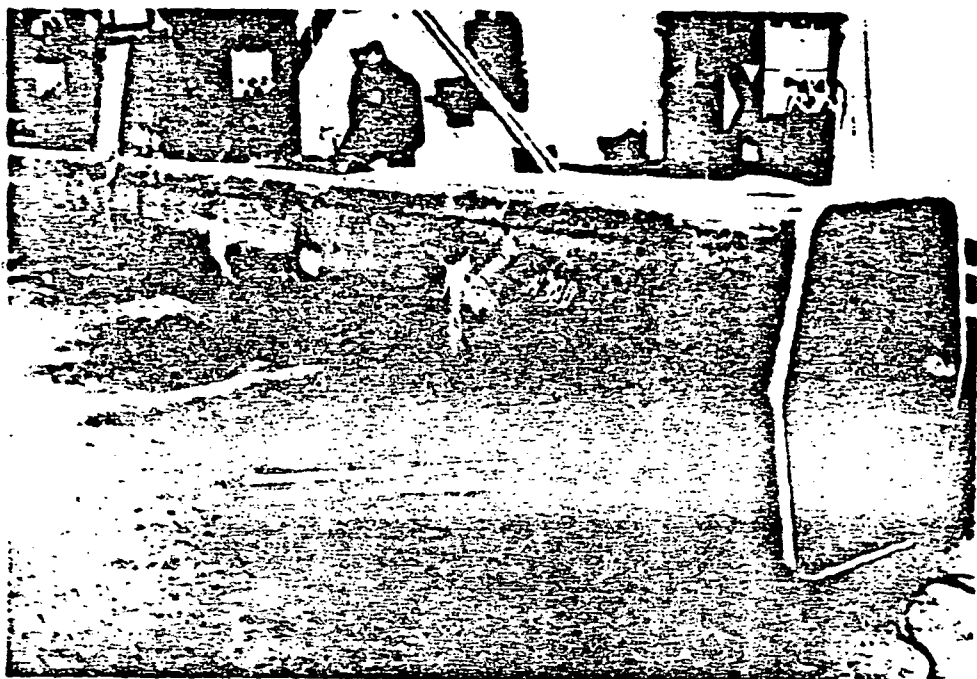


Figure 5: Spar sections R 21.5 to R 35 attached

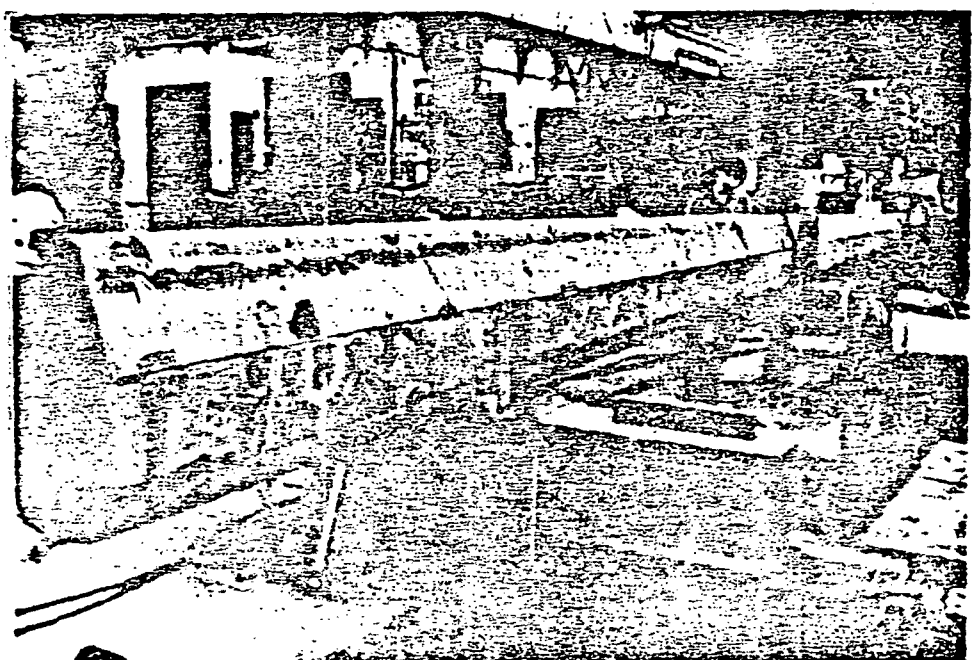


Figure 6: Spar sections R 35- R 50 (stitched together)

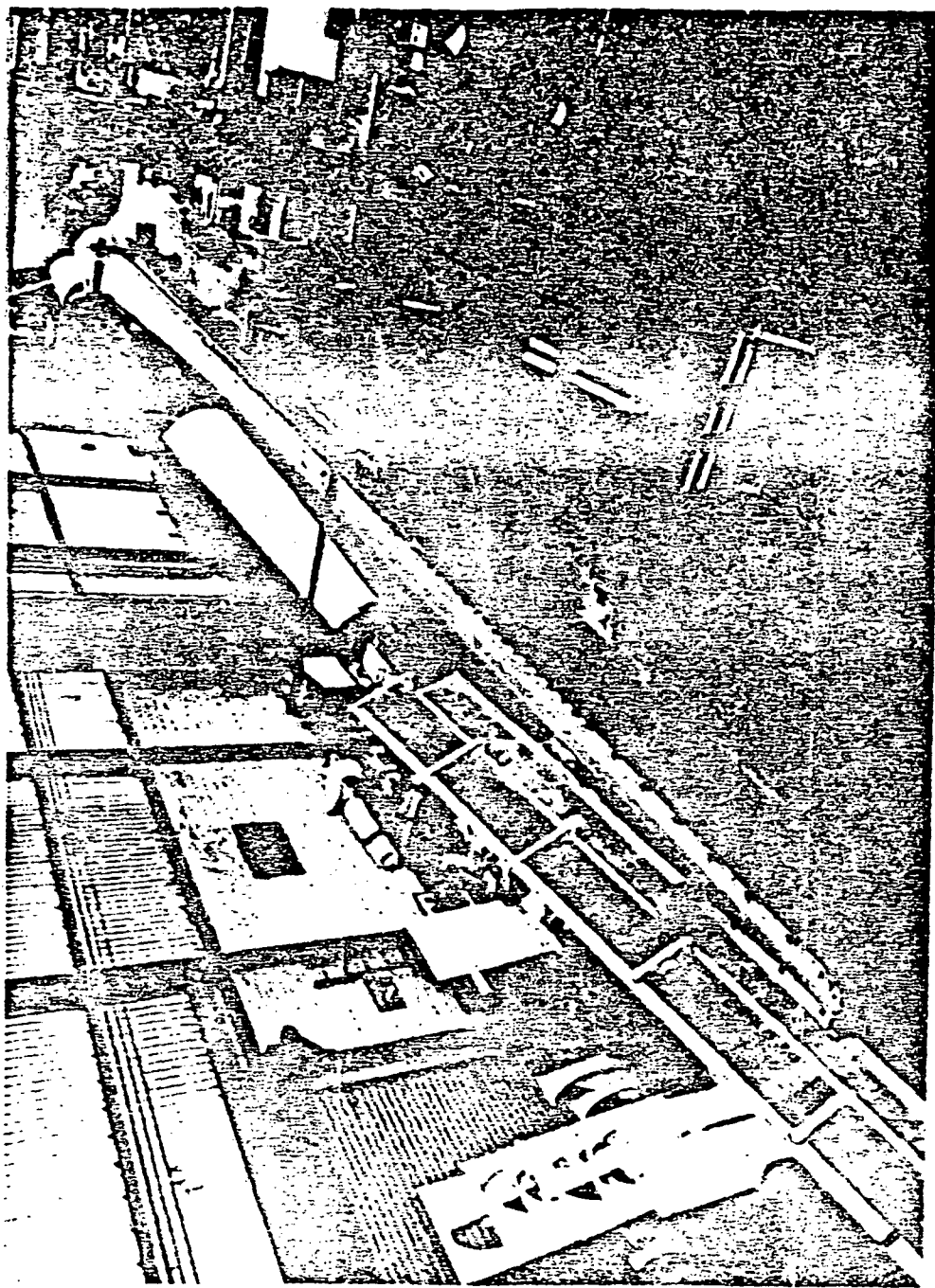


Figure 7: Steel box spar complete with fittings

The shell sections of the GFP sandwich structure of the blade outer skin are fabricated in negative shape molds, a procedure which is conventional and proven in plastics manufacture.

First, a master model of the rotor blade geometry, following the rotor blade span, had to be constructed. (Figure 8). Then, the negative shape mold for the upper and lower shells were shaped from this master model (Figure 9). The separation plane between upper and lower shell is also the wing chord. Since on fabrication engineering and handling grounds one could not manufacture the complete blade skin, it was divided into 5 structural sections, each of which represents a surface of equal size.

The actual manufacture of the shells takes place by manual procedure with vacuum suction. After emplacement of a separator, next a UP pre-gel is sprayed into forms as an external coating, and then the individual glass fabric layers are inlaid according to the coverage plan and impregnated with the matrix. After preparation of the cover laminate of the shell, the reinforcing material is installed in the form of hard foam plates and the entire mold is sealed airtight with a suction foil. A vacuum is created in the mold with a vacuum pump, which induces a contact pressure among the individual layers of glass fiber, together with the reinforcing materials. Any overflowing of resin goes through the holes in the perforated hard foam. (Figure 11)

After a hardening time of 24 hours, the inner laminate is installed and hardened. Following this, the prefabricated ribs of the end box are cemented into the lower shells, and the finished shell is now unmolded (Figure 12).

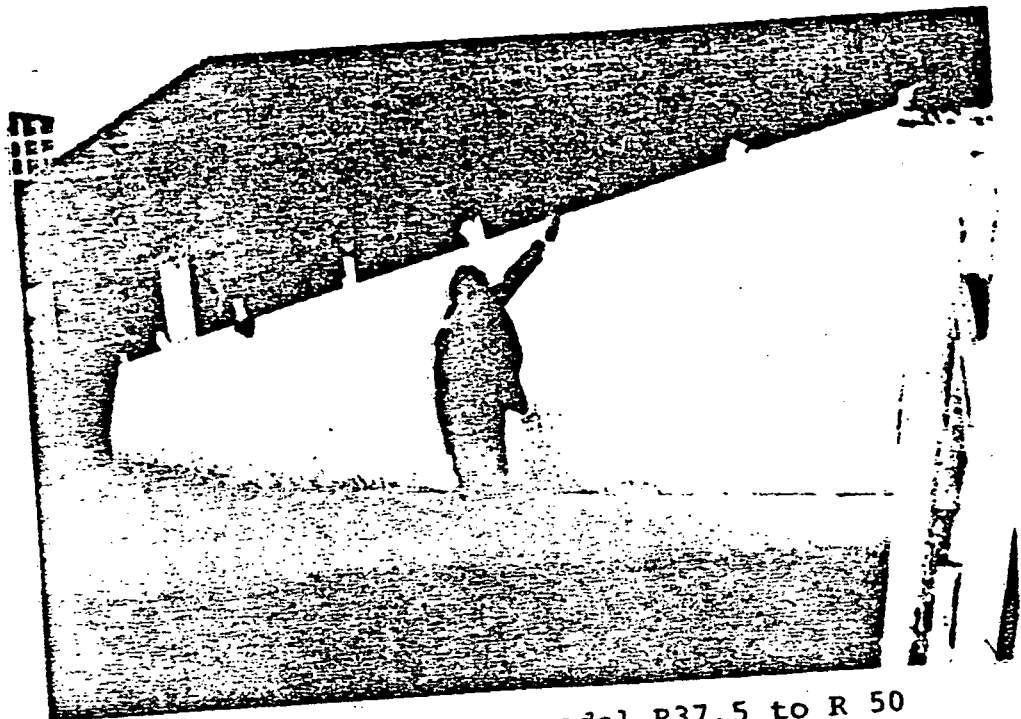


Figure 8: Master model R37.5 to R 50

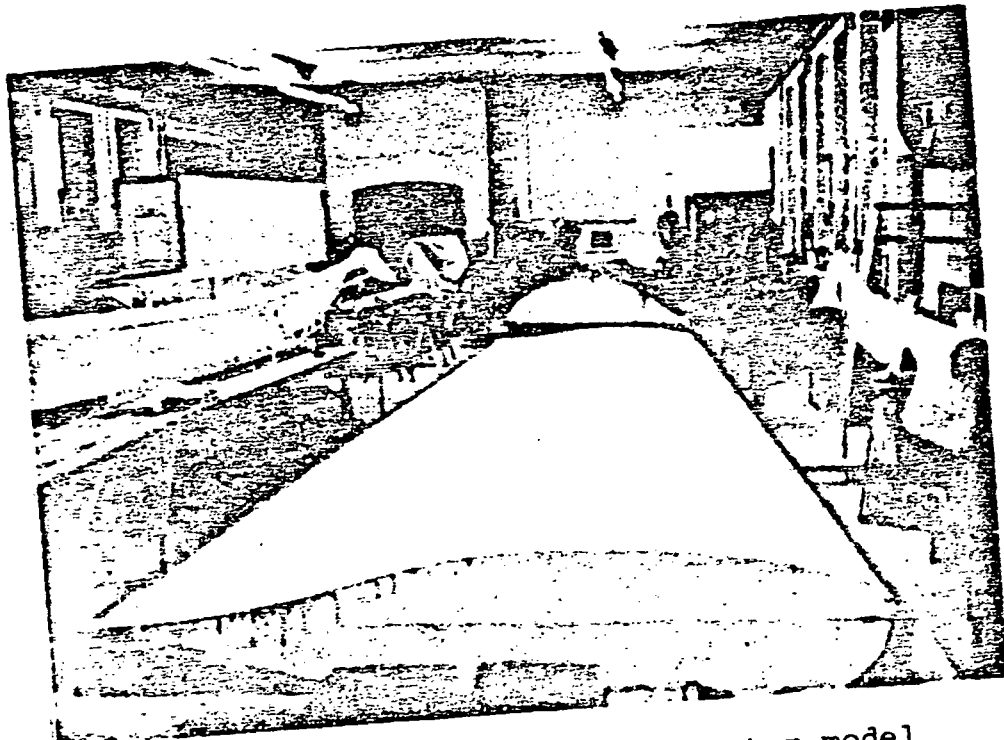


Figure 9: Shape mold with master model

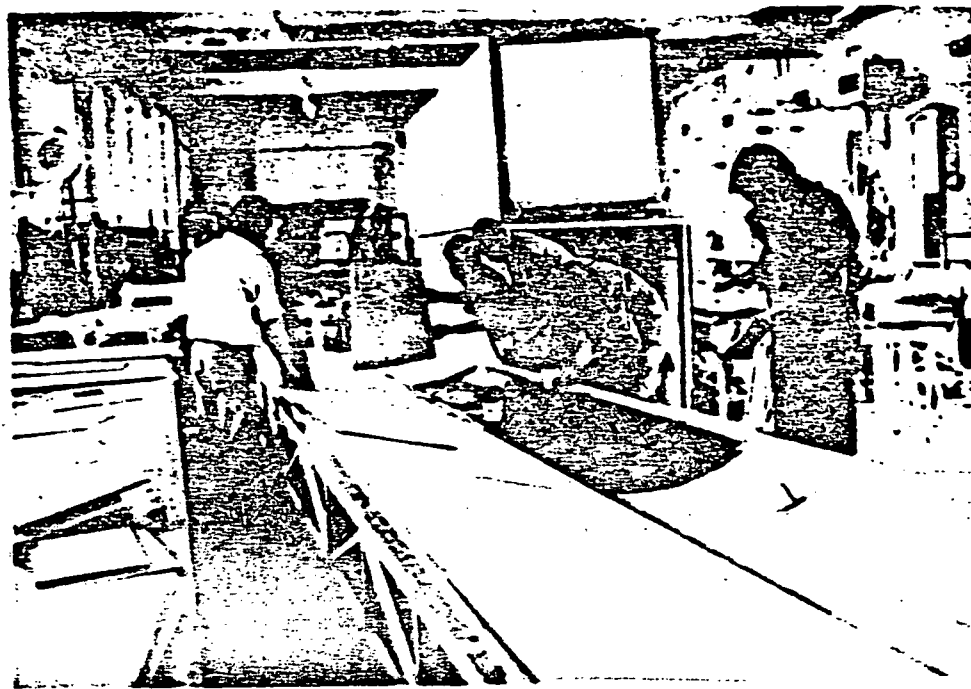


Figure 10: Laminating the shells

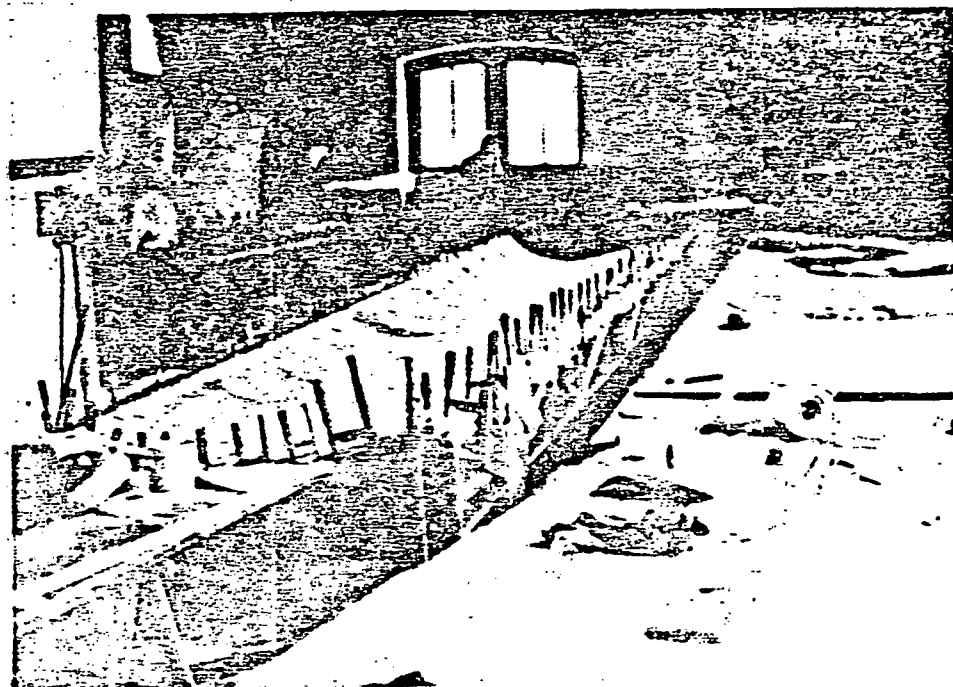


Figure 11: Vacuum generation during the hardening process

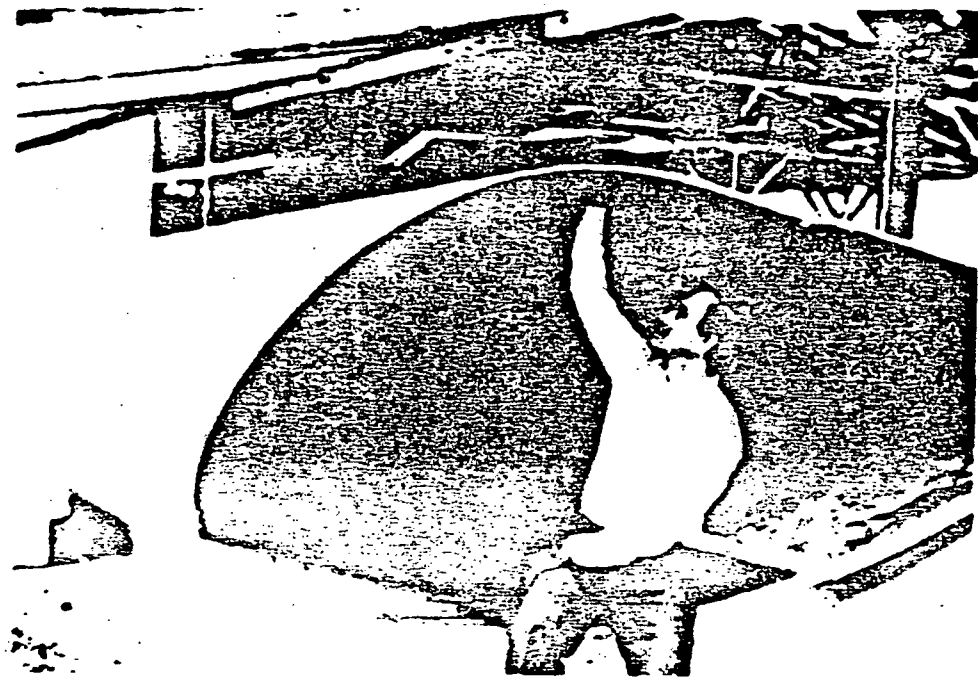


Figure 12: Shell assembly

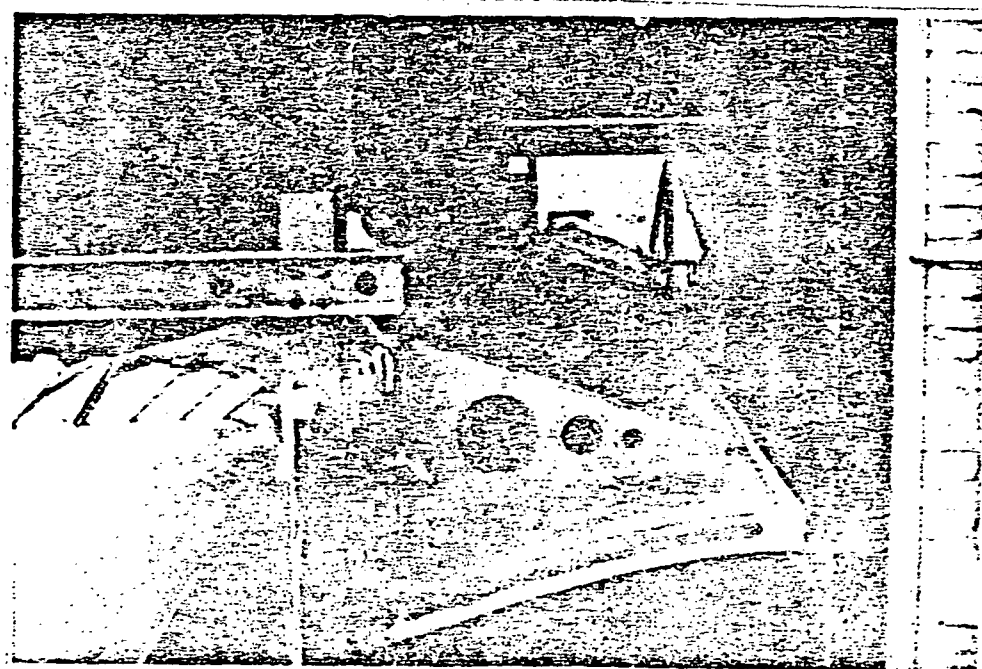


Figure 13: Mounting of the shells

4.3 Mounting

For the mounting of the outer skin, the spar is mounted on stands at various blade stations such that the blade axis runs in a level plane and to avoid, to the greatest extent possible, bending as a result of the spar's own weight.

The starting point was structural section I (R 50- R 37.5) of the blade skin where the lower shell is properly located and adjusted and then bolted and cemented to the spar fittings. After this, the upper shell is mounted and cemented. The procedure is repeated for structural sections II-IV. When all structural sections have been finally mounted, the junction points are smoothed, ground and painted. (Figure 13)

After completion of the blade (Figure 14), the overall geometry is adjusted with help of the templates. Recesses for transport framework and covering on the blade root are installed and enclosed after this assembly is completed.

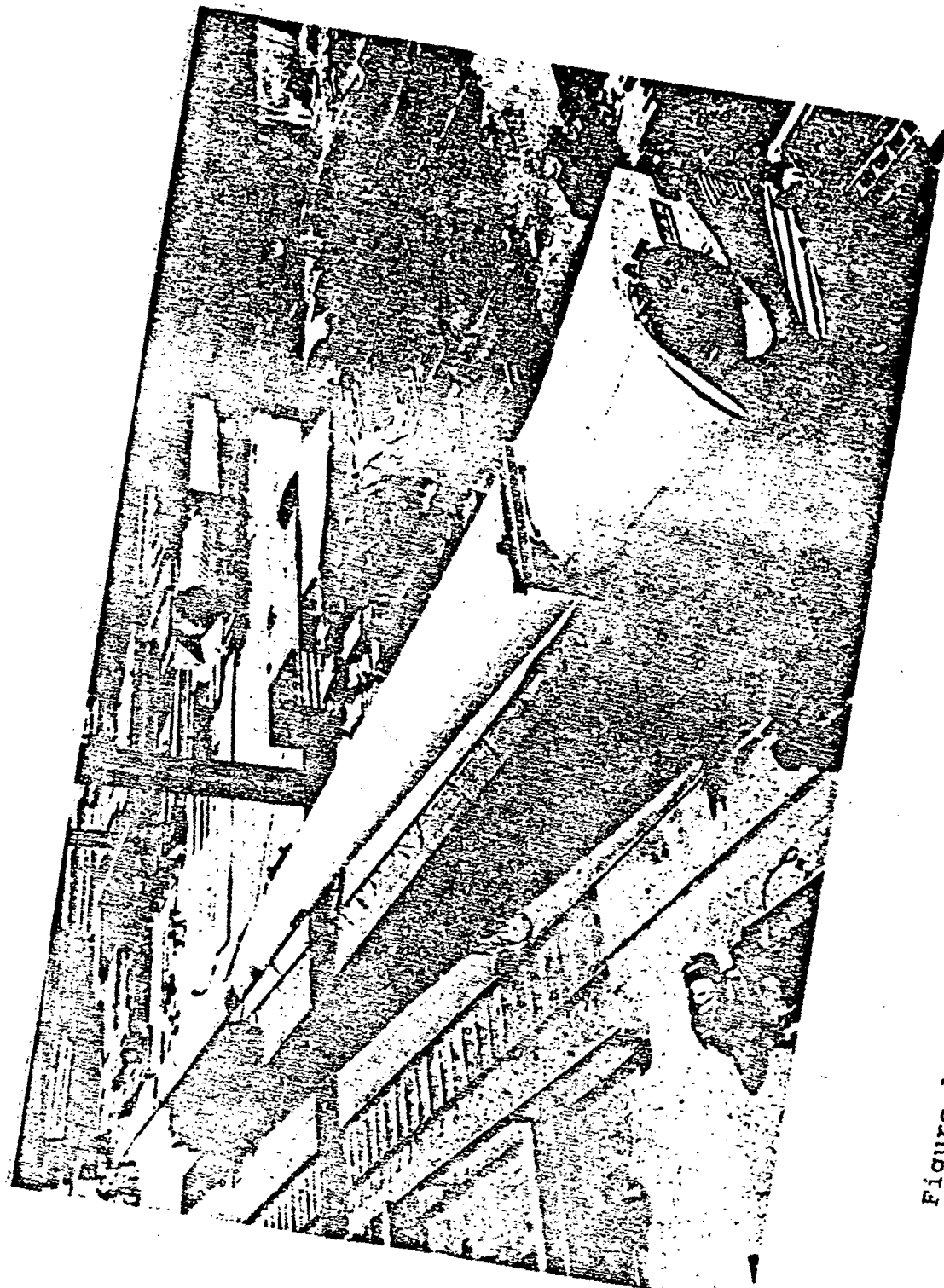


Figure 14: Completed rotor blade

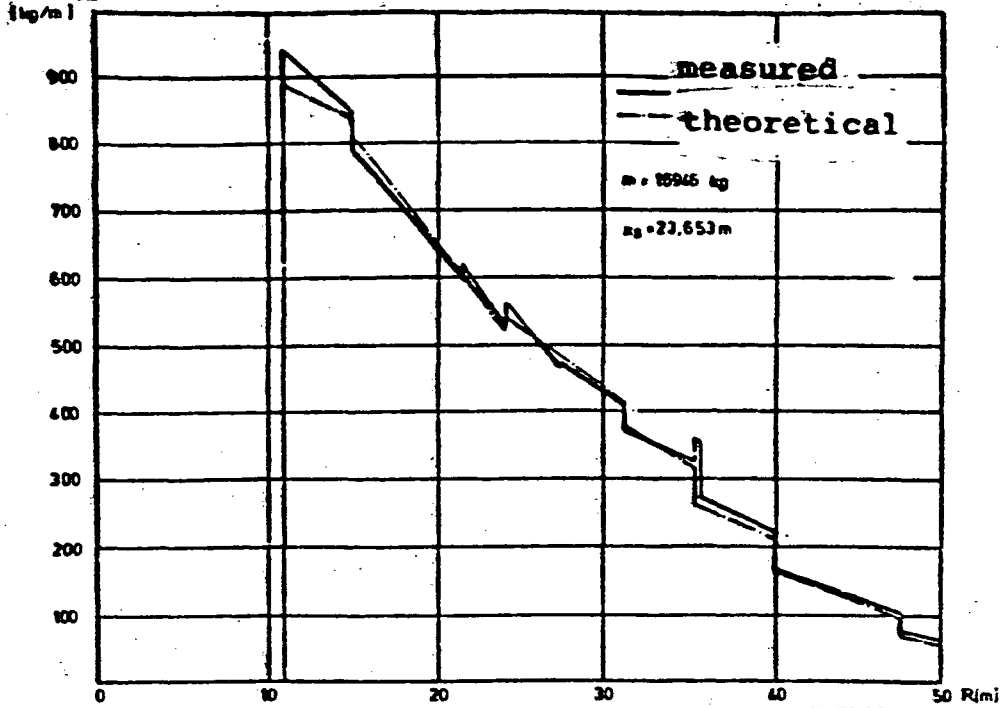
5. QUALITY ASSURANCE

The quality assurance measures are set forth in the Quality Plan /7/, and these were monitored by MAN-NT and the firm German Lloyd Hamburg; the latter also checked the design documentation.

Basically it was required that all materials used be certified with a plant acceptance certificate per DIN 50 049-3.1B which documents structural changes arising during fabrication and reconciles the preparation of the blades with the definition documentation.

More in detail, on the spars all transverse junctions were checked 100% with X-rays and for cracks, and in the case of longitudinal welds, 10% were X-rayed from both seam ends. All process parameters in the welding were continuously checked. In addition, endurance stability tests were carried out on welded surface test articles which had been executed under the fabrication conditions applying to the spar. The findings showed that with an applied load of 2×10^7 a permissible stress amplitude of (illegible symbols) = $\pm 62 \text{ N/mm}^2$ was achieved. For the roughness case K0, the DIN 15 018 yields (illegible symbols) = $\pm 57 \text{ N/mm}^2$. Thus higher stability values were achieved as are laid down as a basis for the stability certification. During manufacture of the shells particular monitoring was done of the maintenance of process parameters such as temperature, air humidity, hardening times and vacuum pressure. Additionally, laminate test articles were produced in parallel to the manufacture of the shells and under the same fabrication conditions in order to confirm the stability values attained.

In order to derive the mass distribution and the location of the center of gravity of the finished blades, during the fabrication all spar sections and shell sections were weighed and also their centers of gravity determined from these measurements. The results of these measurements are shown in Figures 5.1 and 5.2. On account of the differing measurement equipment for rotor blades 2 and 3, blade 2 was balanced by the installation of additional mass in the inner blade area.



/55/

Figure 5.1: Mass distribution on rotor blade 3

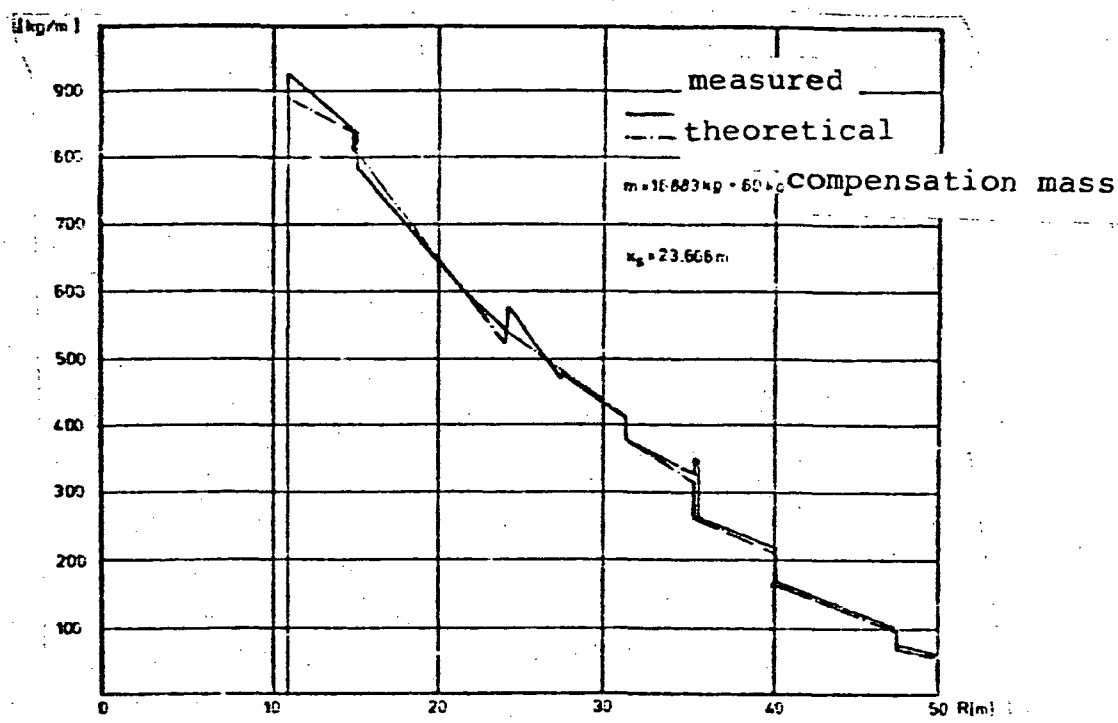


Figure 5.2: Mass distribution on rotor blade 2
(translation note: title assumed from context)

6. TRANSPORT

Despite its immense dimensions, transport of the rotor blade does not present all that great a problem. The prototype was transported from Mainz to Munich/Ottobrunn by truck on the autobahn.

The tractor-trailer combination consisted of the tractor and two steerable trail vehicles with counterpoise pivoted bogie. At blade stations R15m and R 43m the blade was moved by two cranes, in the hoisting and transport slings affixed there, onto the trail vehicles. Between these support points, the blade hung free in the shock direction. The vehicle speed was limited to 40 kph in order to avoid undesirable oscillations. (Figure 15)

Highway transport is also planned to Kaiser Wilhelm Koop.

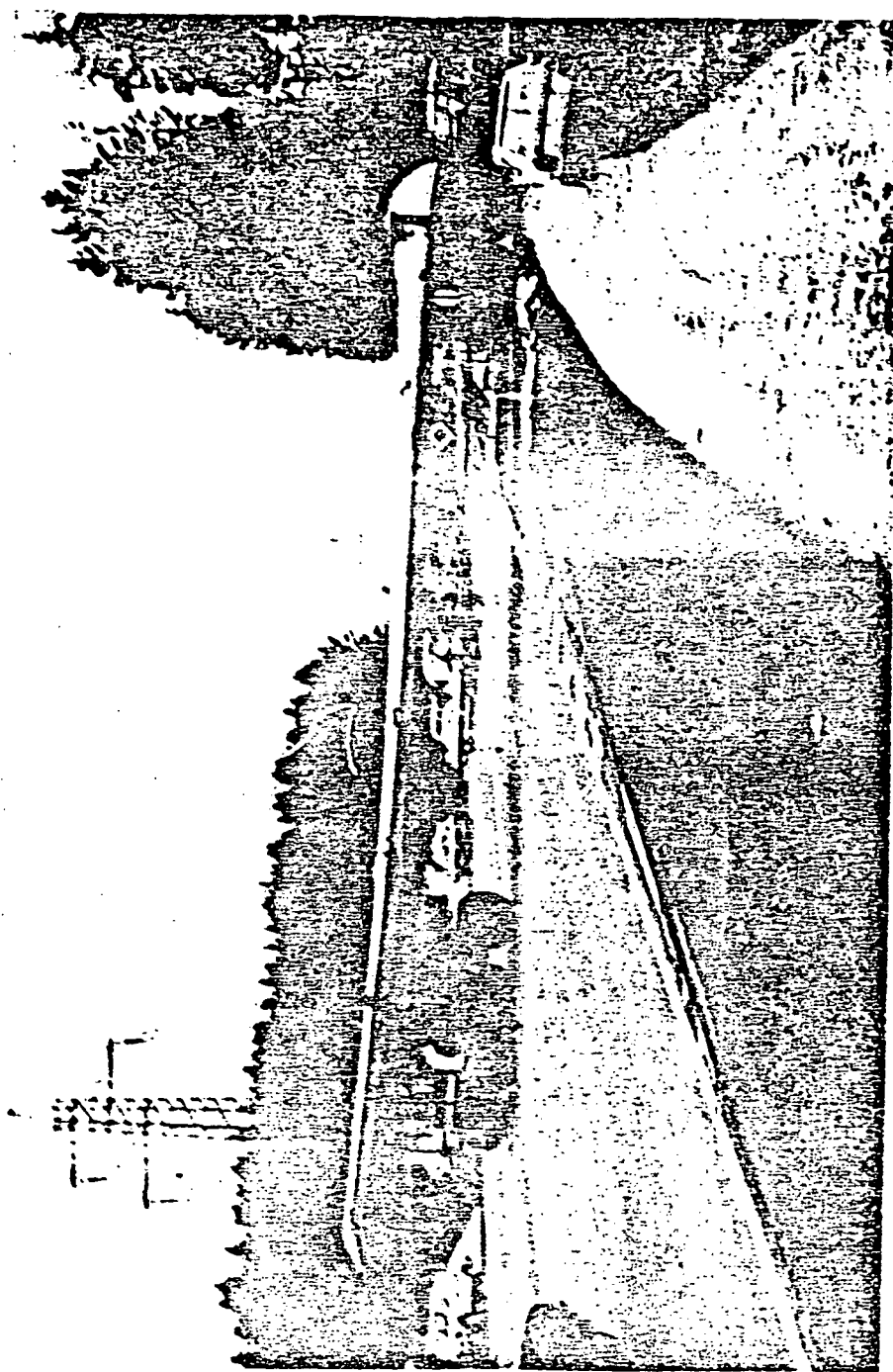


Figure 15: Transport of the test rotor blade

7. TESTING

The prototype of the rotor blade was subjected to static load tests. Dynamic load tests with 10^8 load cycles could not be carried out due to the large amplitudes and on scheduling grounds. The test concept aimed at simulating as nearly as possible the load stresses arising at defined, critical areas of the blade. The objective of these structural tests was to produce the experimental qualification certification for the blade structure and the mode of construction chosen. Additionally, using the measurement results it should be established to what extent agreement with the computed values could be supported here.

The following tests were carried out:

- bench oscillation test to derive characteristic oscillation values
- static load test in load case 1.3 (nominal operation)
- rotation test in load case 1.3 to derive the bearing friction moment
- derivation of the inherent weight component in load case 2.5
- static load test in load case 2.5 (negative extreme gust)
- dynamic load test, load case 2.5 (50 load cycles)
- fracture test in load case 2.5

The large dimensions of the test article made necessary a test setup outdoors, which, after installation had taken place, was covered over with a tent.

As test setup, a concept was chosen in which the test equipment, in this case a reinforced concrete foundation, test article and

stress load facility, consisting of hydraulic cylinders, all form a closed system, in which aside from the inherent weight no external reaction forces occur.

Rotor blade including blade bearing was constrained on the foundation frame as cantilever such that the most realistic mounting conditions were realized (Figure 17).

During the tests, elasticities were measured at 450 points /59/ on the spar structure of the blade skin and blade root. The deformation measurements were restricted to 7 blade stations and moveable and fixed bearings of the blade support. All measured data were recorded and stored by an EDP setup.

Analysis of the measured data at the conclusion of the tests showed a fairly good agreement with pre-computed data. Using measurements from blade station R 27.5, the stress readings for load cases 1.3, 2.5 and the fracture load case are reproduced here (Figures 7.1 to 7.6) /9,10/.

In figures 7.7 to 7.9 can be seen the rotor blade deformations for the respective maximum test loads, without, however, the inherent weight component. Figures 18-21 show the setup for the individual structural tests. In the final fracture test, at 170% of the safe load (load case 2.5), the stresses in some areas of the spar did not show a linear character, whereupon the test was ended. The dynamic test in load case 2.5 with 50 load cycles showed no evidences of fatigue in the structure.

In addition to the structural tests with the test rotor blade, a series of investigations have been carried out on the spar/skin airfoil points as well as endurance stability tests on welded flat test articles. The welded flat specimens achieved altogether better

values with respect to KO per DIN 15 018 with 10^7 load cycles (see Section 5).

In the case of investigations of the skin/spar airfoil points, endurance stability tests checked a skin segment fastened to the spar trailing edge in two planes consecutively with 50% overload and in each case 2×10^7 load cycles; no expansion of the bolt holes in the laminate nor cracks could be determined /8/.

In addition, the blade skin has been bombarded with 20mm ice pellets in order to be able to determine the damage from hailstorms. The impact velocity was between 30 and 148 m/sec (Figures 22,23).

With ice pellets of 20mm Ø, minor delaminations occurred at velocities between 40 and 100 m/sec; below 40 m/sec no damages were determined.

Ice pellets of 10mm Ø showed minor delamination only above 120 m/sec /8/.



Figure 16 Test stand foundation



Figure 17 Blade mounted on the test stand foundation

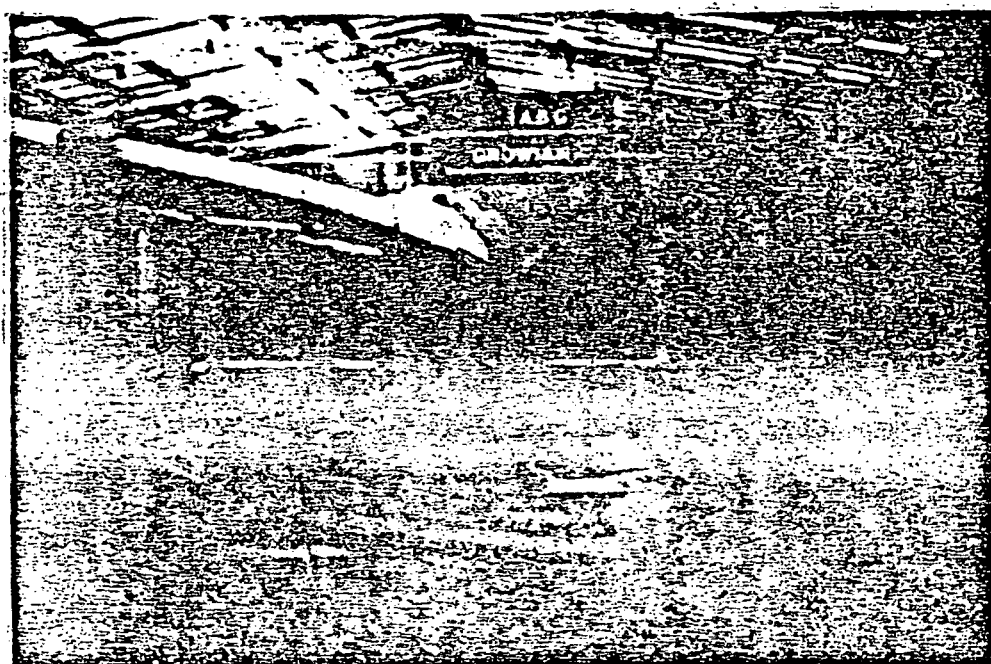


Figure 18 Bench oscillation test

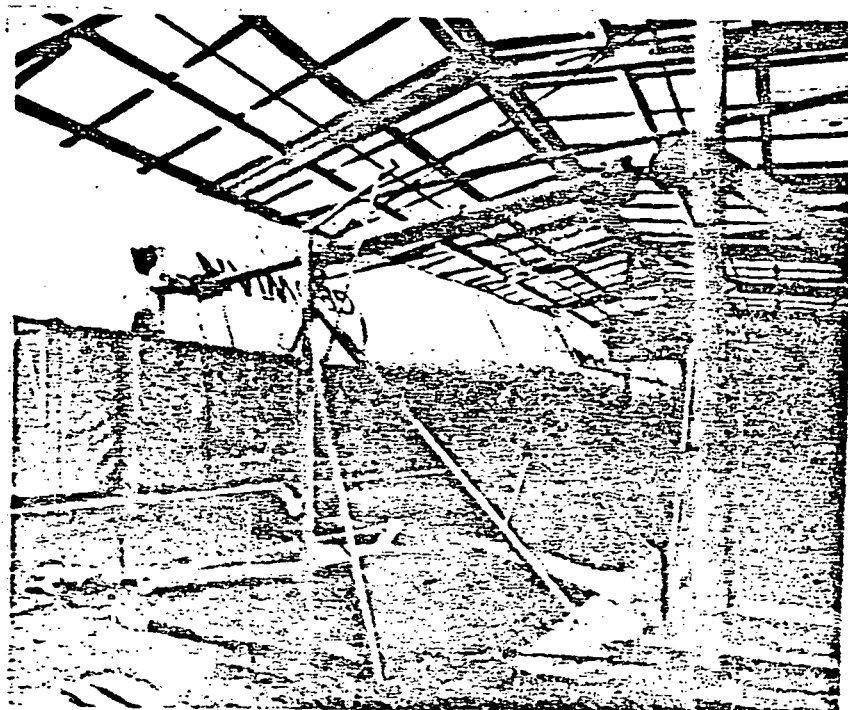


Figure 19 Test setup for load case 1.3

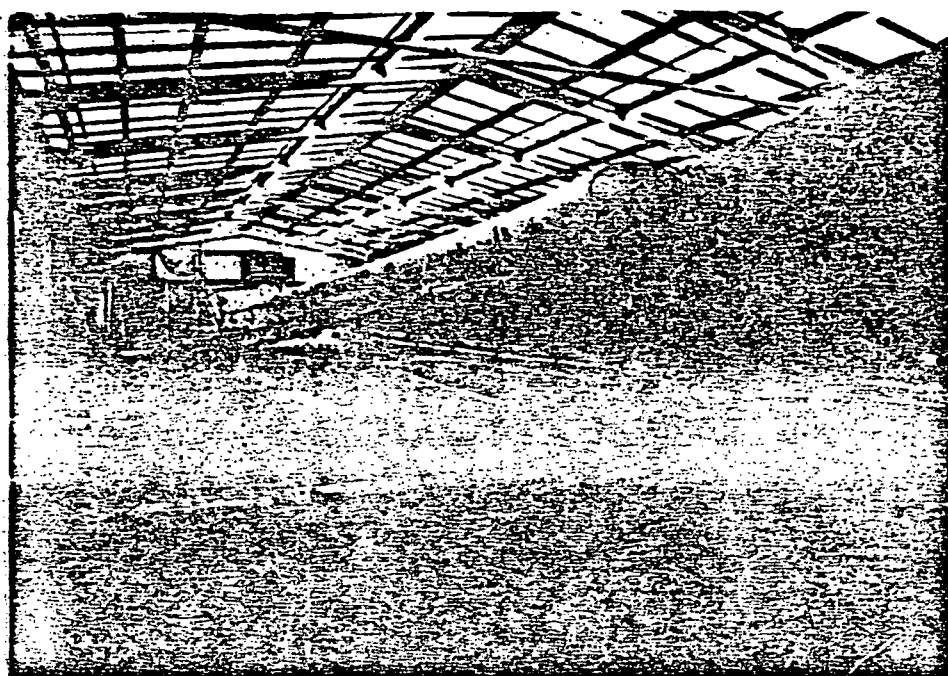


Figure 20 Test setup for load case 2.5

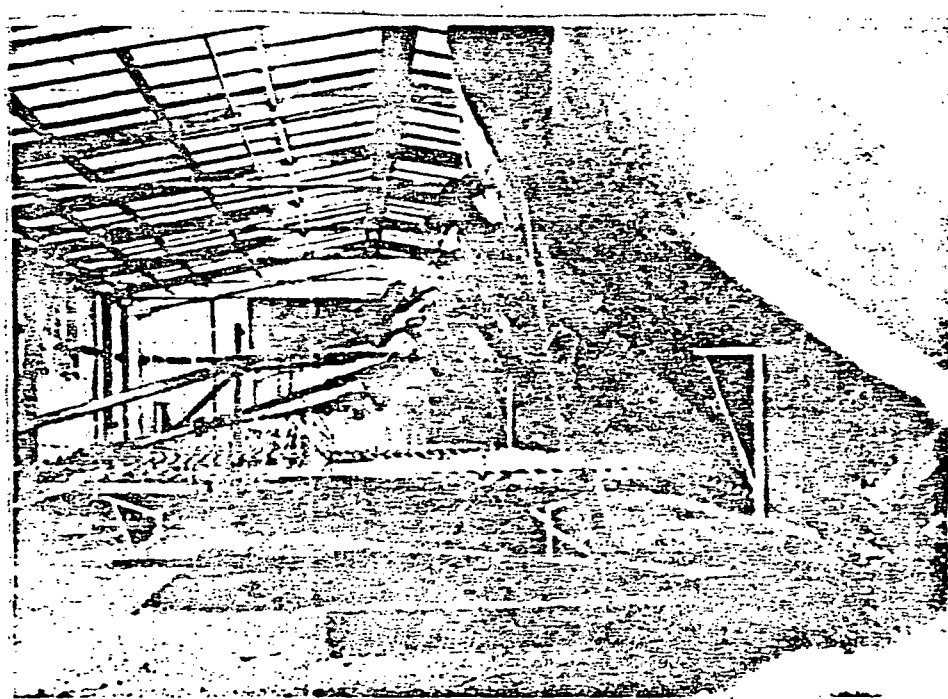


Figure 21 Fracture load case

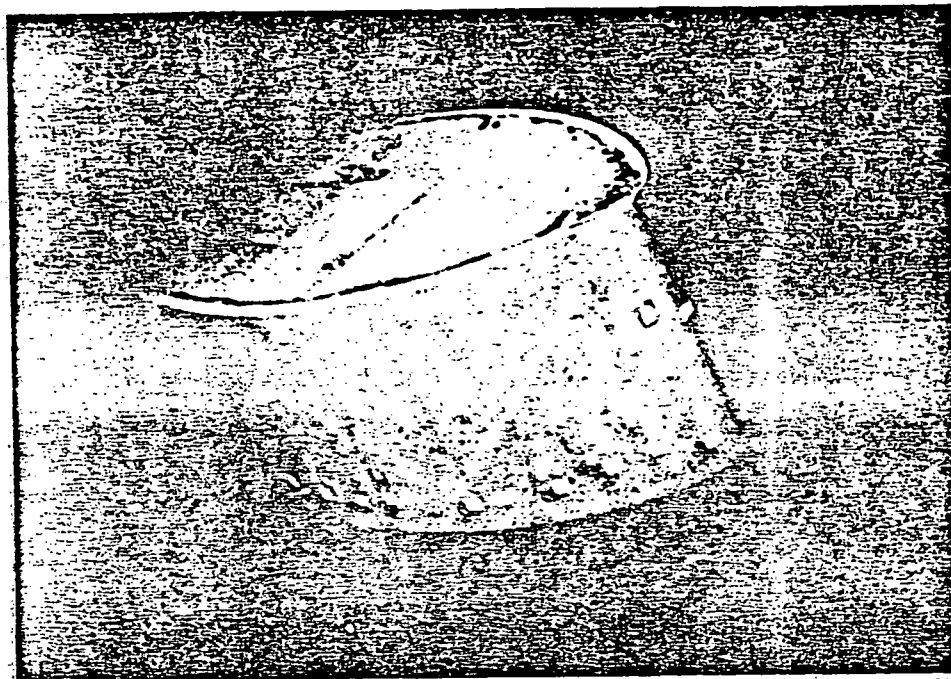


Figure 22 Test article for hail impact tests

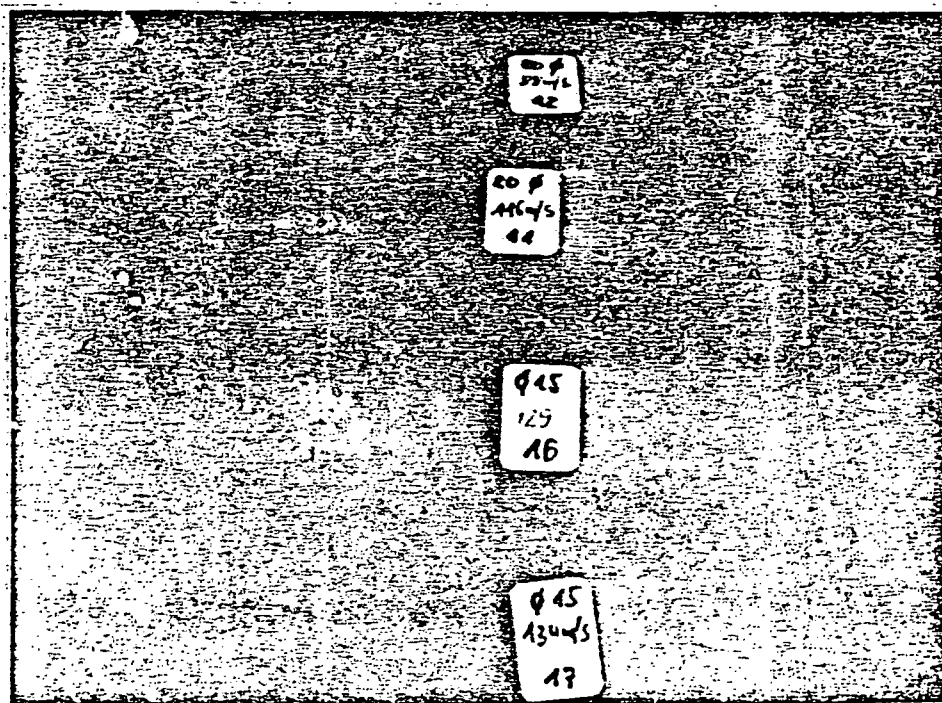


Figure 23 Blade skin damage from hail impact tests

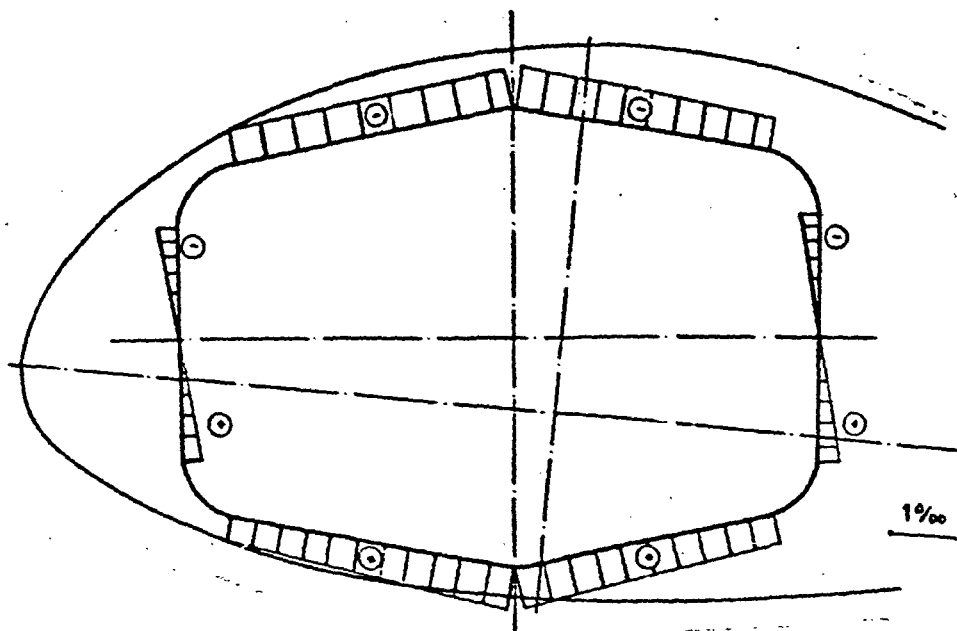


Figure 7.1 : Spar stretching in cross-section
R 27.5 in load case 1.3

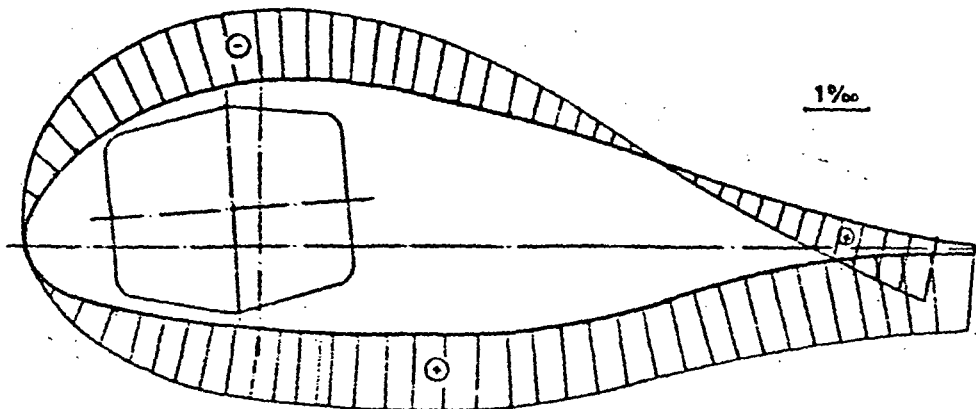


Figure 7.2: Longitudinal stretching in the blade skin
as a result of spar deformation in load case 1.3

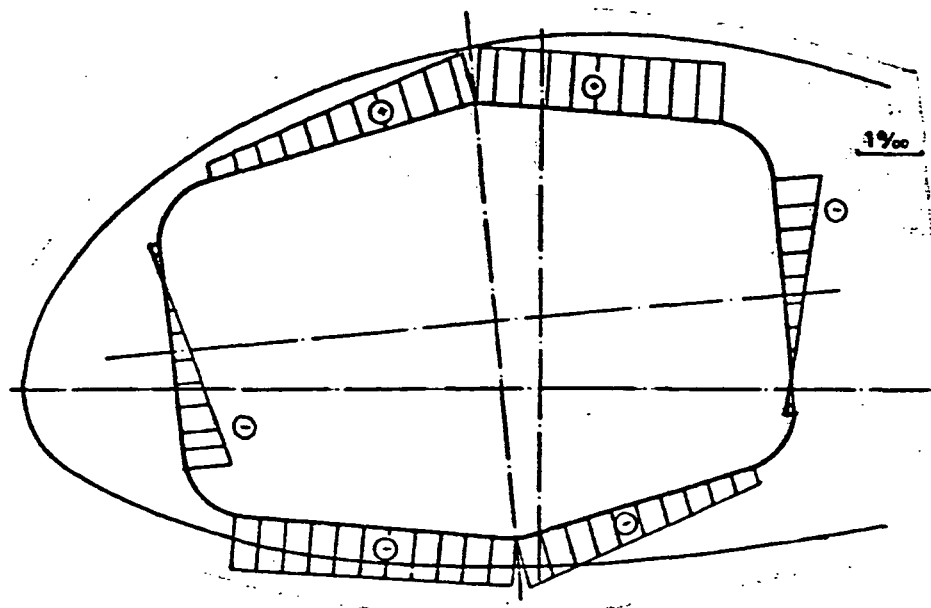


Figure 7.3: Spar stretching in cross-section R 27.5
in load case 2.5

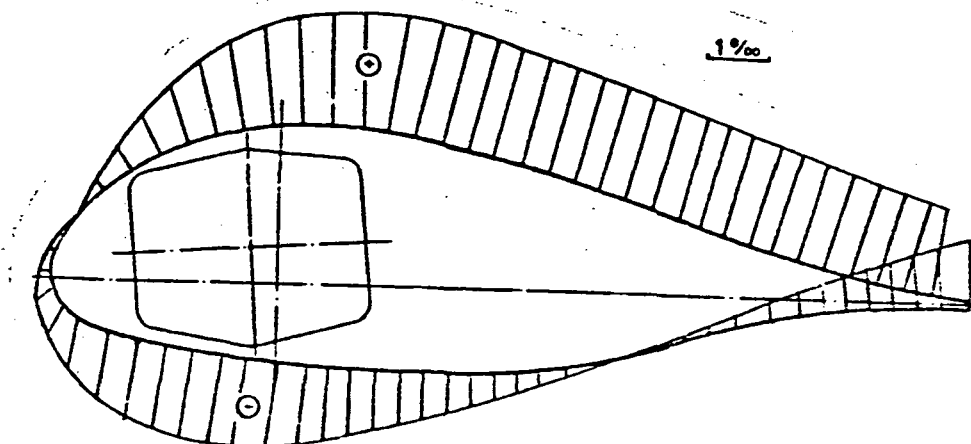


Figure 7.4: Longitudinal stretching in the blade skin as a
result of spar deformations in load case 2.5

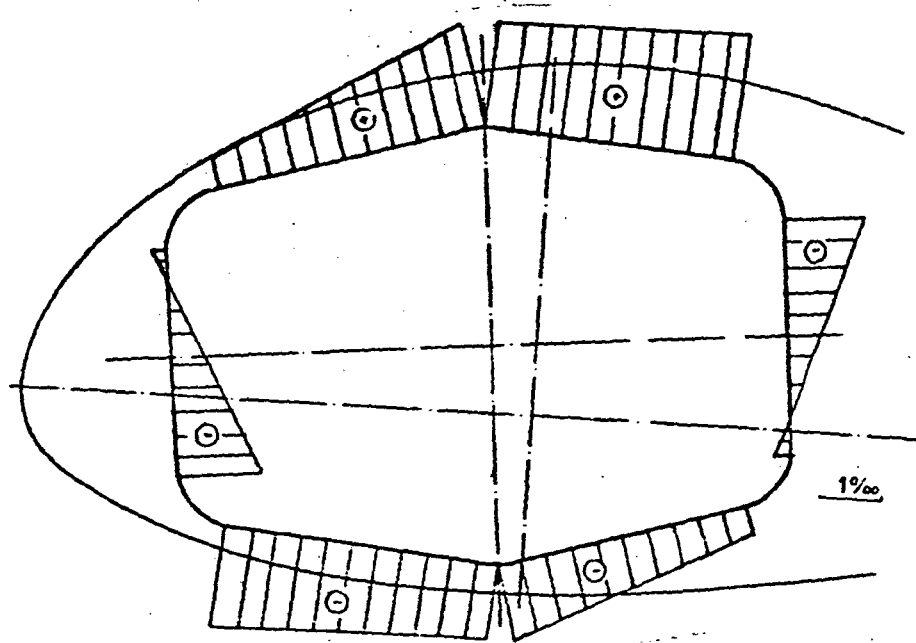


Figure 7.5: Spar stretching in cross-section 27.5 in the fracture load case

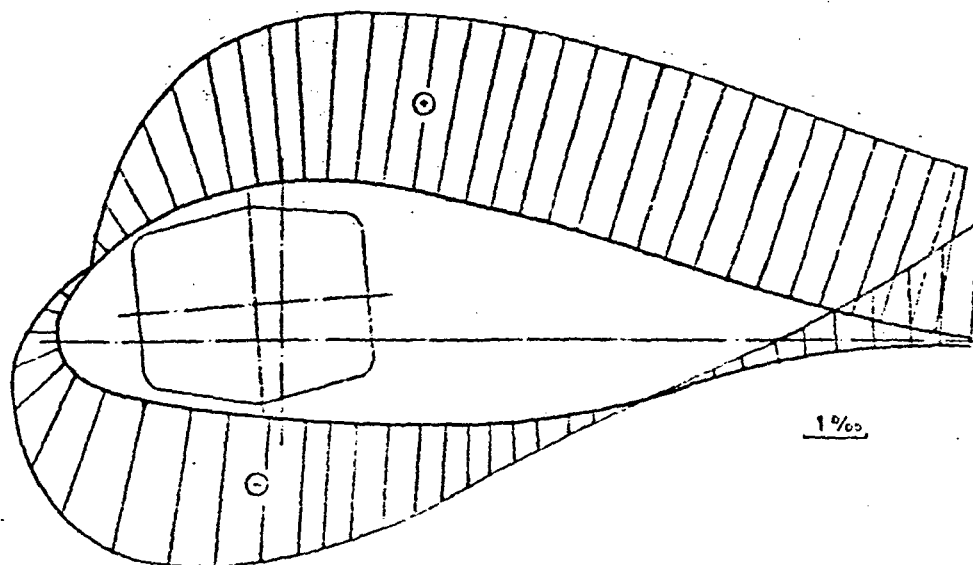


Figure 7.6: Longitudinal stretching in blade skin as a result of spar deformation in fracture load case R 27.5

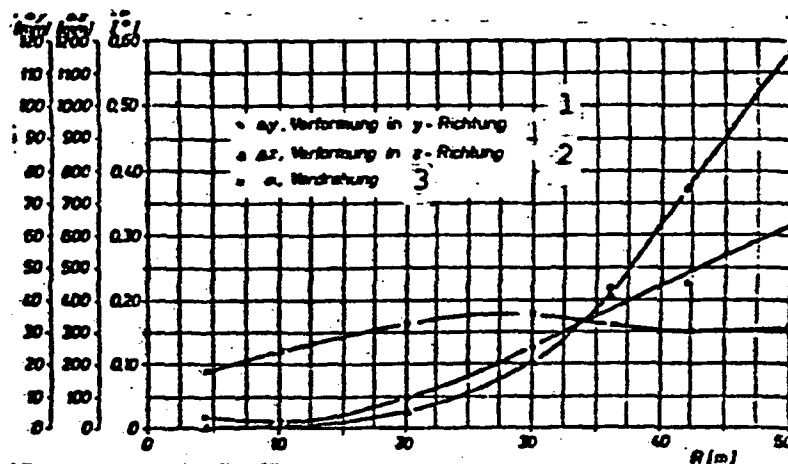


Figure 7.7 : Blade deformation in load case 1.3

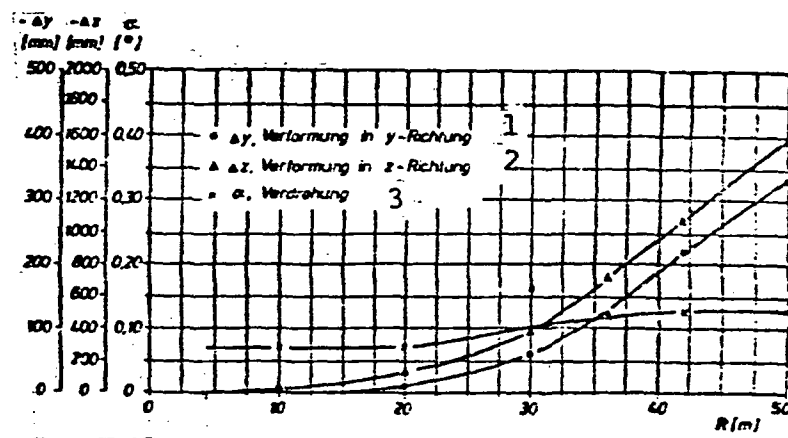


Figure 7.8 : Blade deformation in load case 2.5

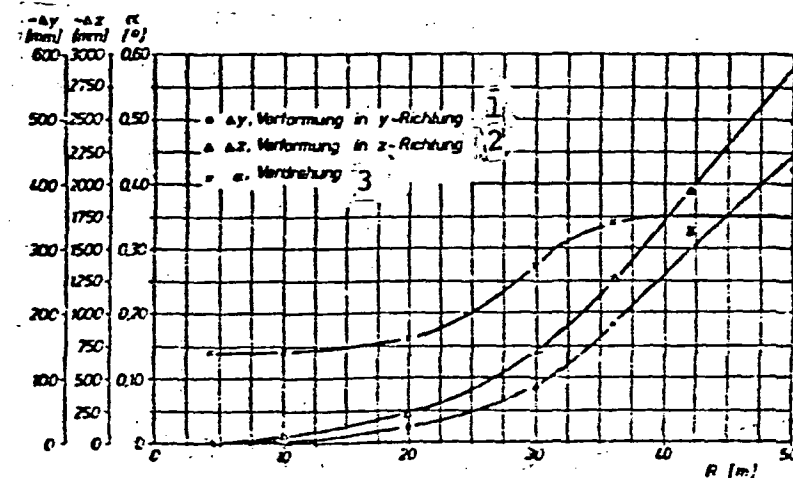


Figure 7.9 : Blade deformation in fracture load case

1. deformation in y-axis
2. deformation in z-axis
3. twisting

Table 3: Comparison of the blade characteristic frequencies measured in test and the computed values

Characteristic form	f [Hz] measured	f [Hz] computation
1. Schlag	0.923	0.956
2. Schlag	2.39	2.64
3. Schlag	4.66	5.22
4. Schlag	8.03	9.08
5. Schlag	12.11	13.95
6. Schlag	17.38	19.53
7. Schlag	23.86	27.10
1. Schwenk	1.27	1.27
2. Schwenk	3.55	3.64
3. Schwenk	7.40	7.54
4. Schwenk	13.02	13.47
5. Schwenk	19.91	21.20
1. Torsion	21.67	26.16

shock
twisting rotation

8. PROJECT EXECUTION

In addition to MAN-NEW TECHNOLOGY, which carried out the project management, design, construction and computations on the rotor blade, the MAN plants at Gustavsburg and Nürnberg were concerned with the fabrication of the steel structural components. The firm of Schempp-Hirth, Kirchheim/Teck was responsible for the design and production of the GFP shell of the blade skin. Structural tests with the test rotor blade were carried out by Industrial Plant Operating Co. (IABG), Ottobrunn. The firm German Lloyd was entrusted by the KFA-Juelich with checking on the design and computational documentation and on the fabrication of the rotor blades. Figure 8.1 clarifies the project organization.

8.1 Schedule

Preparations for this project began in January 1979. From the letting of the contract in July 1979 until September the final blade geometry was decided so that construction of equipment and forms for the steel spar and the blade skin could take place. In March 1980 the slipway for the spar and the negative form molds for the GFP shells were completed and construction of the test rotor blade began which was completed at the end of January 1981.

In parallel with the fabrication of the test rotor blade, the test stand equipment for the structural tests and the blade root structure with blade bearing and test stand attachments were completed. In February 1981 the test rotor blade was installed in the test rig and in March 1981 the tie-down oscillation test was carried out.

Static load stress testing could be started in mid-May after installation of the stress load facility and the extensive measuring instrumentation; this ended in mid-July 1981 with the fracture testing.

The fabrication of both rotor blades for the first GROWIAN installation took place in the time period March 1981 to July 1982. In Figure 8.2 is portrayed the time course of the individual work packages of the project.

PROJECT ORGANIZATION

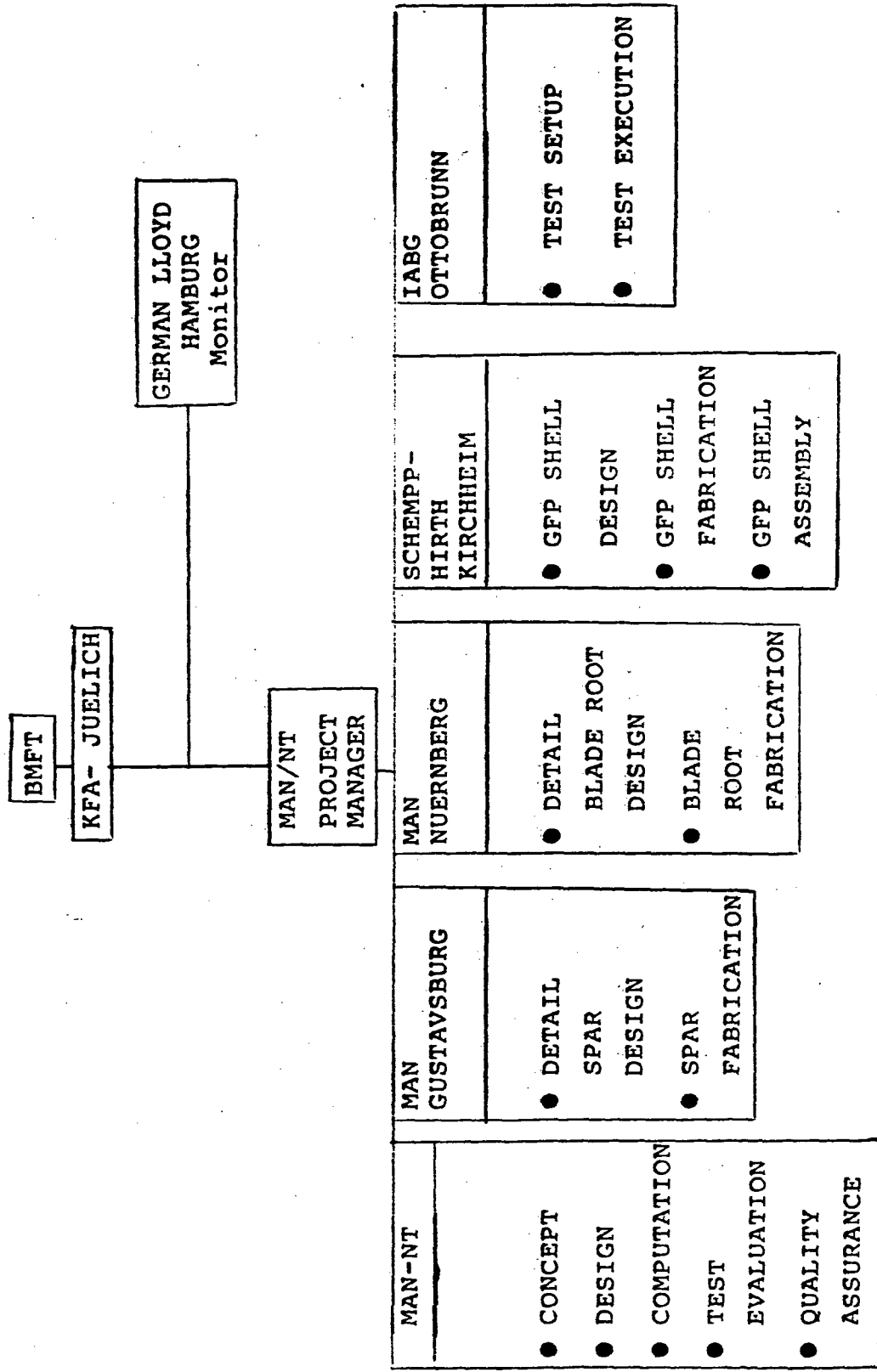


Figure 8.1 Project Organigram

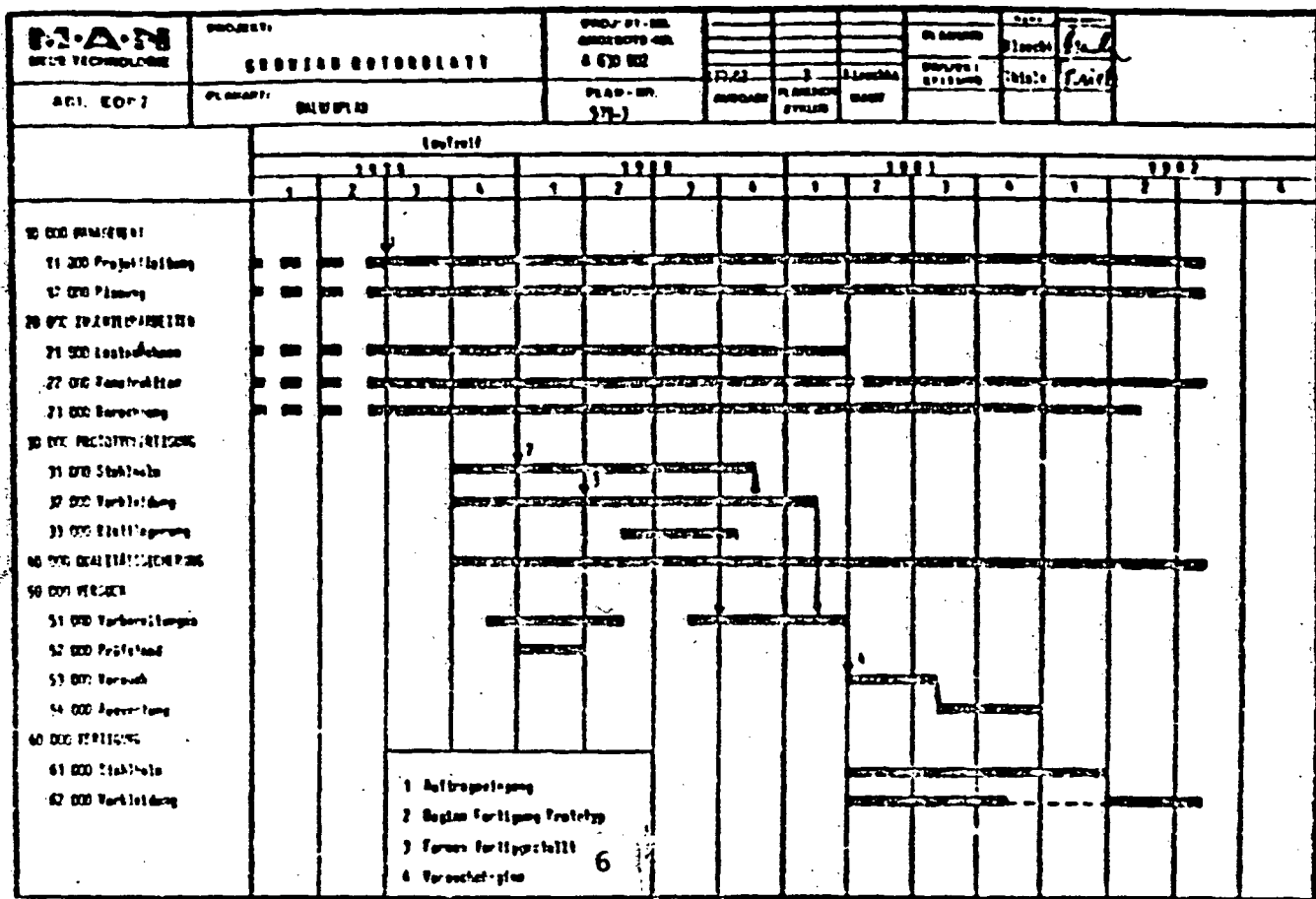


Figure 8.2 Milestone Plan

1.	MANAGEMENT	4. (CONTD) TESTING
	Project management	?
	Planning	Test stand
2.	? TASKS	Test
	Load assumptions	Evaluation
	Design	5. FABRICATION
	Computation	Steel spar
3.	PROTOTYPE FABRICATION	Sheathing
	Steel spar	6. Contract let
	Sheathing	Begin prototype fabrication
	Blade ?	? completed
4.	QUALITY ASSURANCE	Begin testing
		TRANSLATOR NOTE: Work copy has many illegibilities ?

8.2 Resource Expenditure

The development of the rotor blade, construction of three blades and the structural testing with the test rotor blade required outlays of DM 10.3 million which were divided as follows among the individual items:

1. Rotor blade development (engineering)	30%
2. Equipment construction	11%
3. Fabrication of 3 rotor blades	42%
4. Testing	<u>17%</u>
TOTAL	100%

9. CONCLUSIONS

It was demonstrated with the construction of three rotor blades that rotor blades for wind power plants with a rotor diameter of 100m can be built using the chosen concept with reasonable expenditures.

Despite the use of simple fabrication tools, the very narrow fabrication tolerances--considerably less than those usual in steel work--could be met on both spar and blade root. In the course of the fabrication of the steel box spar it appeared that the weld seams which lie crossways to the load direction should be carried out with particular care in order to experience no diminution of the endurance stability. This seems to be an important criterion for the construction of rotor blades of this great size with welded steel structures since in normal production of weld seams, the blade mass would be considerably increased and would rapidly reach the practical limit. For the most part this also applies for rotor blades with a profile contour trued steel spar, although here the cross-sectional geometry available can be better utilized.

In manufacturing the GFP shells for the blade outer skin it could be determined that with an appropriate subdivision of the shells into fabrication sections of equal size, the manual laminating process can be carried out and the desired surface quality can be achieved. However, in the future a more temperature resistant resin system should be employed, although to be sure such a one is not yet available on the market.

With respect to future repetitive production with larger numbers of items, stamping machine tools should be manufactured for fabrication of the spar shells in order to reduce the tedious measuring and adjustment work and to enhance the quality. For the shells, insofar as possible, mechanization of the fabrication should be striven for, e.g. automatic wetting of the E-glass fabric with the resin preparation and mechanical cementing of the fabric strips. By these and similar measures shortening of the work times and improvement in the quality would be made possible. Further improvement looking to the optimization of the blade structure can first be undertaken after operational experience with GROWIAN and in particular after availability of the blade stresses measured during operation.

/1/ R. Pernpeintner Aerodynamische Rotorblattauslegung von GROWIAN
(Aerodynamic Rotor Blade Concept for GROWIAN)
AV-A 630 802 - ERS-1-013

/2/ G. Huss Aerodynamische Lastannahmen für die GROWIAN Rotor-
blätter (Aerodynamic Load Assumptions for the GROWIAN
Rotor Blades) SS-W 705 081-01

/3/ G. Sukarie Festigkeitsbericht für die GROWIAN-Rotorblätter (Stability
Report on the GROWIAN Rotor Blades) MAN-NT-Report
NR 22/81

/4/ K. Kehl Dynamische Rotorbelastungen (Dynamic Rotor Stresses)
W. Keim A 300 132 - EDS - 040

/5/ G. Sukarie Symmetrische Eigenfrequenzen der GROWIAN Rotorblätter
Symmetrical Characteristic Frequencies of the GROWIAN
Rotor Blades) A 630 802 - EGS - 017

/6/ D. Ludwig Eigenschwingungs- und Flatterrechnungen am GROWIAN
E. Klusowski Rotorblatt (Computations of Characteristic Oscillations
and Flutter on GROWIAN Rotor Blades)
DFVLR 1B 232 - 81 C 21

/7/ J. Köhler Qualitätssicherung GROWIAN MAN-NT Komponenten (Quality
Assurance on GROWIAN MAN-NT Components) SS-W 705 081 - 004

/8/ H. M. Thiele GROWIAN-Rotorblatt Untersuchungen von Flügestellen
D. Muser (Investigations on Junction Points on the GROWIAN Rotor
Blade) MAN-NT Report No. 33/81

/9/ Rödlmeier Strukturversuche am GROWIAN-Rotorblatt (Structural Testing
of the GROWIAN Rotor Blade) JABG-Report No. B-TF-1227

/10/ G. Sukarie H. G. Ströhle	Auswertung der Strukturversuche am GROWIAN-Rotorblatt (Analysis of the Structural Tests on the GROWIAN Rotor Blade) MAN-NT Report No.
/11/ P. Agatonovic	GROWIAN-Rotorblatt Grundlagen des Betriebsfestigkeitsnachweises (GROWIAN Rotor Blade, Bases for the Operating Stability Certification) MAN-NT Report No. 4/81
/12/ E. Hau, G. Huss	Lastannahmen GROWIAN Definition der Lastfälle (Load Assumptions for GROWIAN Definition of the Load Cases) SSW 709 081-001 Part I

SPECIFICATIONS

SU-W 705 081-318 (02)	GROWIAN Steel Spar Rotor Blade
SU-W 705 081-319 (05)	GROWIAN Rotor Blade -Test Program
SU-W 705 081-320 (01)	GROWIAN Rotor Blade Span
SD-W 705 081- 322 (3)	GROWIAN Rotor Blade Acceptance
SD-W 705 081-324 (02)	GROWIAN Rotor Blade Materials
SD-W 705 081-325 (01)	GROWIAN Rotor Blade Transport and Handling
SD-W 705 081-326 (0)	GROWIAN Rotor Blade Lightning Protection
SS-W 705 081-004	Quality Assurance for GROWIAN MAN-NT Components

MAN-NT- STANDARDS

/76/

E-FN 379 (01)	GROWIAN Rotor Blade Fabrication scheme-Aerodynamic Casing
E-FN 380 (01)	GROWIAN Rotor Blade Installation Scheme for Aerodynamic Casing
E-PN-421	GROWIAN Rotor Blade Testing in Shell Fabrication
E-QN 322	Rough Plate from QSt 52-3, Special Quality Z3 (GROWIAN)
E-TL 381	Rough Plate from QSt 52-3, Special Quality Z3 (GROWIAN)
E-VN 379 (01)	Corrosion Protection of GROWIAN Rotor Blade Steel Spar by Coatings
E-VN- 382	GROWIAN Rotor Blade-Installation of Blades
E-FN- 374	Installation of GROWIAN Rotor Blade Prototype on the Test Stand
FA-G-SP-80.1	GROWIAN Rotor Blade- Weld Scheme
B72.61 006-1001	Test Instruction Steel Spar R10.85-R27.5m
B72.61 006-1002	Test Instruction Steel Spar R 27.5-R50.12
161 006 1001/1002	Spar, Fabrication Scheme
DRAWINGS	
Drawing set No.	94.008 76 0000